RM L57L13

NACA

RESEARCH MEMORANDUM

TESTS OF AERODYNAMICALLY HEATED MULTIWEB WING STRUCTURES

IN A FREE JET AT MACH NUMBER 2

FOUR ALUMINUM-ALLOY MODELS OF 20-INCH CHORD AND SPAN

WITH 0.064-INCH-THICK SKIN, 0.025-INCH-THICK

RIBS AND WEBS, AND ZERO, ONE, TWO, OR

THREE CHORDWISE RIBS

By John R. Davidson, Richard Rosecrans,
and Louis F. Vosteen

Langley Aeronautical Laboratory
Langley Field, Va.

NATIONAL ADVISORY COMMITTEE
FOR AERONAUTICS
WASHINGTON

May 8, 1958

NATIONAL ADVISORY COMMITTEE FOR AERONAUTICS

RESEARCH MEMORANDUM

TESTS OF AERODYNAMICALLY HEATED MULTIWEB WING STRUCTURES

IN A FREE JET AT MACH NUMBER 2

FOUR ALUMINUM-ALLOY MODELS OF 20-INCH CHORD AND SPAN

WITH 0.064-INCH-THICK SKIN, 0.025-INCH-THICK

RIBS AND WEBS, AND ZERO, ONE, TWO, OR

THREE CHORDWISE RIBS

By John R. Davidson, Richard Rosecrans,
and Louis F. Vosteen

SUMMARY

Four multiweb wing models were tested at a Mach number of 2 in a
free jet to investigate structural effects of aerodynamic heating and
loading. The models had a 20-inch chord and span; a 5-percent-thick,
circular-arc airfoil section; and three, two, one, or zero chordwise
internal stiffening ribs. Each aluminum-alloy model had 0.064-inch-
thick skins, six 0.025-inch-thick spanwise webs, and 0.025-inch-thick
tip bulkheads. The model with no internal ribs survived the first test
at sea-level static pressure and a stagnation temperature of 93° F, but
failed during the second test at a stagnation temperature of 563° F.
The other models survived all tests. Temperature and strain measurements
were made on all models and the data were tabulated. Calculated stresses,
determined from the temperature distribution on the model with one rib,
are compared with the stresses determined from measured strains. The
tests showed that the addition of a single rib maintained sufficient
structural integrity to prevent flutter after loss of stiffness caused
by thermal stress and reduced modulus of elasticity at elevated tempera-
tures. Modes determined from laboratory vibration tests without heating
show that the addition of only one rib nearly doubles the lowest frequency
at which cross-sectional distortion occurs.

INTRODUCTION

This is part of a series of reports describing tests conducted by the Langley Structures Research Division to investigate the effects of combined aerodynamic heating and loading on built-up wing structures. Aerodynamic heating can reduce structural stiffness by lowering material moduli and inducing thermal stresses. Previous papers (refs. 1 to 4) describe the tests on the first seven models in this series. The first model (model MW-1) was of 40-inch chord and semispan and failed during a test in which the structure was subjected to aerodynamic heating. The second model (model MW-2) was essentially a half-scale version of model MW-1 and had a 20-inch chord and semispan; this model also failed under similar test conditions. Both models were tested at a Mach number of 2 and a stagnation temperature near 500° F, and both developed flutter involving cross-sectional distortion which ended with the destruction of the models. Additional tests were made on models of the MW-2 design to obtain pressure data and to investigate the effect of angle of attack on the flutter mode. (See ref. 5.) Model MW-4 differed from model MW-2 only in the thickness of the tip bulkhead (0.025 inch thick for model MW-4 and 0.250 inch thick for model MW-2); model MW-4 failed in a manner similar to that of models MW-1 and MW-2. The remaining models (MW-3, MW-5, MW-6, and MW-7) survived similar tests.

The flutter and failure of models MW-2 and MW-4 indicated the need for additional initial stiffness to maintain sufficient structural resistance to flutter after aerodynamic heating had lowered the material moduli and thermal stresses had changed the stiffness of the built-up wing structure. (See refs. 6 and 7.) Consequently, the design of model MW-4 was modified by the addition of one, two, and three chordwise ribs in models designated MW-18, MW-17, and MW-16, respectively. In addition, another model identical to model MW-4, and designated MW-4-(2), was included in the test program covered in this report. These models were tested to measure model temperature and strain distributions, to confirm the previous conclusion that aerodynamic heating contributed to the failure of model MW-4, and to evaluate the effectiveness of chordwise ribs in preventing distortion of the cross section. The effects of chordwise ribs are discussed, and an attempt is made to correlate measured stresses with calculated stresses.

SYMBOLS

R   radius, in.

T   temperature, °F

T*   normalized temperature, °F; $T_b^* = \dfrac{(T_t - T_o)_a}{(T_t - T_o)_b}(T - T_o)_b + T_{o,a}$

T_t stagnation temperature, °F

T_o initial temperature (model), °F

α   angle of attack, deg

Subscripts:

a   test conditions experienced by model MW-18 during its first
            test

b   test conditions or model temperatures under consideration

   Stress, expressed in psi or ksi, is positive for tension and is
negative for compression.

MODELS

Model Construction

   Each semispan wing model had a 5-percent-thick, symmetrical, circular-
arc airfoil section and was constructed from 2024-T3 aluminum alloy with a
20-inch chord and $24\frac{1}{8}$ - inch span of which $19\frac{7}{8}$ inches extended into the air-
stream. Internal construction consisted of six 0.025-inch-thick spanwise
webs spaced $2\frac{1}{2}$ inches apart and three, two, one, or zero 0.025-inch-thick
chordwise stiffening ribs with the number depending upon the particular
model. All models had a 0.025-inch-thick tip bulkhead, 0.064-inch-thick
skin, and solid leading and trailing edges. At the base of each model
there were two 0.081-inch-thick doubler plates, a $2\frac{1}{2}$ - inch-thick root
bulkhead, and two 1/2-inch-thick-steel clamping blocks for attaching the
model to its supporting structure. Aluminum-alloy standard and blind
rivets were used throughout. Sketches of each model showing individual
construction details are found in figure 1. A photograph of the interior
of model MW-16 prior to final assembly is shown in figure 2.

   The model exteriors were painted with zinc chromate primer, upon
which a black India ink grid was superimposed to help determine model

motions and deformations from motion-picture data. The effect of this
paint on the heat transfer into the structure is small. (See ref. 4.)

Instrumentation

All models were instrumented with iron-constantan thermocouples with
the beaded junctions peened into small holes drilled into the skins, webs,
and ribs. Thermocouples mounted in the interior of the solid leading- or
trailing-edge sections were first coated with cement and were then inserted
into small holes drilled into these sections. Figure 3 shows the thermo-
couple locations for each model.

Figure 3 shows the locations where SR-4 type EBDF-7D temperature-
compensated wire strain gages were attached to the models with thermosetting
cement. These strain gages are compensated to read approximately zero
strain when used on unstressed aluminum alloy at temperatures between 50° F
and 250° F. The useful temperature range may be extended by first post-
curing the gage cement to the maximum test temperature and then, after
cooling to room temperature, calibrating the gage by slowly heating the
model in an oven while measuring the indicated strain when load and thermal
stresses are absent. The maximum model temperature expected during these
tests was 450° F; inasmuch as heating the model to this temperature would
change the aluminum-alloy properties, the gage cement was postcured to only
250° F and, therefore, gage accuracy was sacrificed to prevent changes in
the material properties. The natural frequency of the galvanometers used
to record strain data was about 100 cps; thus, these galvanometers were not
suitable for measurement of high-frequency strain amplitudes.

The following list gives the estimated probable errors in individual
measurements and the corresponding time constants. The time constant,
which is considered independent of the probable error, is defined as the
time at which the recorded value of a step-function input is 63 percent
of that of the input; after three time constants, the response amounts to
at least 95 percent of the input.

Item	Probable error	Time constant, sec
Stagnation pressure	±0.7 psi	0.03
Stagnation temperature . . .	±3° F	.12
Model temperature	±3° F	.03
Model strain	±150 microinches/inch	.02

Errors due to thermocouple installation have not been included but are believed to be small.

High-speed 16-millimeter motion pictures were taken of each test to record model behavior. The high-speed cameras had a frame rate of 600 to 1,600 frames per second. Monitor cameras running at 120 frames per second were used to augment the data supplied by the high-speed cameras. The cameras and oscillograms were correlated by using a common 1/10-second timing pulse.

APPARATUS AND PROCEDURE

Aerodynamic Test Facility

The tests were made in the preflight jet of the Langley Pilotless Aircraft Research Station at Wallops Island, Va. The preflight jet is a blowdown-type wind tunnel in which models are tested in a 27- by 27-inch free jet at the exit of a Mach number 1.99 supersonic nozzle. A description of the jet operation and characteristics may be found in reference 2.

Disturbances within the jet during the starting and shutdown periods cause violent model oscillations, and for some of these tests a retractable tip stabilizer was used to restrain the model until test conditions were reached. The stabilizer was activated at about 1 second after the start of the air flow, it released the model at 1.3 seconds, and it left the airstream at about 1.7 seconds. Immediately preceding the shutdown period, at about 11 seconds, the stabilizer reentered the airstream and had fully gripped the model at about 12 seconds.

Laboratory Vibration Tests

Prior to the wind-tunnel tests, a vibration survey was made to find the natural modes and frequencies of each of the models. An electromagnetic shaker supplied energy to the model, and the response was detected by a phonograph-type pickup whose signal was fed into a cathode-ray oscilloscope. The frequencies were measured by a Stroboconn frequency meter.

Jet Tests

Figure 4 is a photograph of a typical model mounted on the jet test stand preparatory to an aerodynamic test. An aerodynamic fence surrounded the model base and protected the model instrumentation leads. The sharp leading edge of the fence was raised 1/8 inch above the bottom wall of the jet nozzle to scoop off a small boundary of air. The leading edge of the

model was located 2 inches from the nozzle-exit plane; this separation may have diminished as much as 1/4 inch during a high-stagnation-temperature test because the nozzle expanded toward the model.

All tests were conducted with the model oriented at zero angle of attack with respect to the jet center line.

Model MW-4-(2) was first tested at a stagnation temperature near ambient temperature (93° F) and then at a high stagnation temperature (563° F). Model MW-16 was first tested with the stagnation temperature near ambient temperature; the next three tests were made at elevated stagnation temperatures. The other two models were tested at the elevated temperatures only.

RESULTS AND DISCUSSION

Laboratory Vibration Tests

Vibration modes and frequencies for the models are indicated in table I. The node-line locations for individual model modes varied only slightly from the average locations sketched in this table. The addition of ribs changed mode C from one involving much chordwise distortion into a clear second bending mode, D. For model MW-4-(2), the lowest frequency at which chordwise distortion occurred was 268 cps. The addition of one rib to this design (to give model MW-18) increased the chordwise stiffness sufficiently to eliminate chordwise deflection below 465 cps, as is evident from the mode-pattern change between modes C and D. In all cases, whenever a single rib was added to the basic configuration the model frequency was raised; adding a second rib increased all frequencies again; but the addition of a third rib was accompanied by a decrease in the frequencies for modes A, B, and D, which may indicate that the added mass had more influence than the incremental change in stiffness. The MW-16 design (three ribs) was the only configuration that exhibited a distinct second torsion mode; the other designs seem to have had insufficient ribs to develop this form of vibration. It appears from these room-temperature tests that two chordwise ribs may represent optimum stiffening for a wing of this design.

Jet Tests

Test conditions.- A summary of the averaged test conditions is given in table II, and typical variations of stagnation pressure and temperature with time are plotted in figures 5 and 6, respectively. Test conditions were deemed to exist whenever the stagnation pressure exceeded 100 psia, which was the period from approximately 2 to 11 seconds after air began to flow into the jet. Averaged test conditions were determined from the

area under the quantity plotted against time curves for the 9 seconds during which test conditions existed.

Model data.- Data from the model instrumentation are presented primarily in tabular form, with values given at the even seconds during a test. All data herein are referenced to zero test time which was taken to occur when the static pressure in the jet nozzle 1 inch from the nozzle exit first deviated from ambient pressure. This occurrence is approximately 1.8 seconds before test conditions are reached.

The severe characteristic starting and shutdown disturbances of the jet destroyed some model instrumentation and caused other instruments to be unreliable. There were other instrumentation failures which probably were initiated by the starting shock but in which the instrument finally failed from a combination of heat and random disturbances. A gap was left in the data in the tables whenever an instrument failed or became unreliable.

The temperature data are presented in table III, and the strain data are presented in table IV. The tabulated strain values are the measurements read directly from the records with no corrections for errors caused by model-temperature changes.

Model Behavior

The behavior of the models during each test is summarized in table V and is described in detail in the following discussion. In addition, a motion-picture film supplement has been prepared of the two tests on model MW-4-(2) and of the second test on model MW-18 and is available on loan. A request-card form will be found at the back of this paper on the page immediately preceding the abstract and index pages.

No attempt was made to evaluate the amplitude of the oscillations from the strain-gage records at any time because the inherent instrumentation attenuation would create large inaccuracies in such an analysis. The exact beginning and ending of most of the recorded and observed oscillations were usually difficult to determine; hence, the times listed in the descriptions of the tests are given only to a valid number of significant figures for each respective measurement.

Test 1 of model MW-4-(2).- During test 1, strain gages 10 and 11 showed that model MW-4-(2) vibrated at 65 cps between 1.5 seconds and 1.8 seconds with a very small amplitude; this was after the jet starting disturbances had ceased. This slight movement was not discernible in the high-speed motion pictures. At 8.7 seconds small-amplitude oscillations commenced; strain gage 1 indicated a vibratory frequency of 130 cps. The motion pictures show that the small amplitude increased monotonically

until 9.5 seconds when the vibration stopped. No further motion was
observed until 10.7 seconds when a slight torsional mode developed;
strain gages 10 and 11 indicated a frequency of 80 cps, which changed
slowly to 70 cps by 11.85 seconds. At 11.8 seconds a definite 173-cps
oscillation was indicated by strain gage 1; the motion pictures show
that a small-amplitude torsional vibration started at 10.7 seconds,
reached a peak at 11.6 seconds, and then decayed to an unnoticeable
movement at 12.3 seconds. At 12.5 seconds a torsional mode appeared
and continued until the shutdown period, which started at 12.6 seconds.

Test 2 of model MW-4-(2).- After 1.0 second, the end of the starting
disturbances of test 2 of model MW-4-(2), the motion pictures showed that
a small vibrational mode at 72 cps was present, but it quickly disappeared
in the pictures. However, strain gage 11 showed that a 72-cps vibration
was present until failure. In the motion pictures the model remained
stationary until 7.32 seconds, at which time a 238-cps flutter mode began;
this mode ended with violent and complete destruction of the model. The
wing apparently first vibrated with skin panel flutter, but the amplitudes
were so small that exact modal identification was made difficult. By
7.42 seconds a mode involving chordwise distortion was identified. This
motion became increasingly violent, and at 7.64 seconds the tip rib showed
evidence of crippling failure at the right side of the model at web 4.
(Webs were numbered from the leading edge to the trailing edge.) At the
maximum displacement of this same point from the model neutral center line
at 7.656 seconds, the rear portion of the tip rib was torn from the model.
The next sign of progressive failure occurred at 7.672 seconds when a tear
started at the leading edge near the base of the model. The tear reached
the trailing edge at 7.677 seconds, and the remains of the model were
carried downstream. Photographs of this failure sequence are shown in
figure 7.

Test 1 of model MW-16.- During the period throughout which test con-
ditions existed, no motion of model MW-16 during test 1 was visible in
the motion pictures. Some intermittent small-amplitude oscillations,
probably excited by random jet noise, were indicated by the strain-gage
records. These frequencies were between 60 and 78 cps.

Test 2 of model MW-16.- The strain-gage record of model MW-16 during
test 2 showed some very small amplitude, random oscillations of intermit-
tent duration at 275 to 286 cps from after the starting disturbances until
the beginning of the shutdown period. At 10 seconds strain gage 9 showed
a vibration of increasing amplitude with a frequency of 60 cps which may
have actually started before 10 seconds, but the vibration was not large
enough to cause a noticeable strain-gage signal. At 12 seconds this
motion showed clearly in the motion pictures but died out after 13 seconds.
At 13.3 seconds the shutdown disturbances began.

Test 3 of model MW-16.- The model tip stabilizer was used during the starting and shutdown periods of test 3 of model MW-16. Although the motion pictures showed no visible movement, strain gage 19 indicated that a small-amplitude vibration, 258 to 266 cps, existed throughout the test.

Test 4 of model MW-16.- After the starting period of test 4, model MW-16 remained stable until 9 seconds when strain gage 9 indicated a small vibration at 60 cps which lasted until the shutdown disturbances began. For this test only one camera, operating at about 100 frames per second, was used; this motion could not be seen in these pictures.

Test 1 of model MW-17.- The strain-gage records of test 1 of model MW-17 indicate that some form of disturbance (probably random jet noise in the test house) caused the model to vibrate slightly at frequencies between 130 and 140 cps. After the tip stabilizer reentered the airstream preceding the shutdown period, the model developed a small torsional mode that was visible in the motion pictures. All strain gages indicated a frequency of 140 cps. The motion pictures indicated that the vibrations were intermittent from 10.9 seconds until the shutdown period.

Test 2 of model MW-17.- After the starting period of test 2 of model MW-17, there was no motion until 11 seconds when the tip stabilizer reentered the airstream. Then, a torsional mode developed at 140 cps and continued until the beginning of the shutdown disturbances.

Test 1 of model MW-18.- Model MW-18 remained stationary after the starting period of test 1. At 11 seconds when the tip stabilizer reentered the airstream, a torsional and bending mode of vibration commenced at a frequency of 145 cps which remained until the beginning of the shutdown period.

Test 2 of model MW-18.- Strain gages 11, 12, and 20 indicated some small vibration of model MW-18 during test 2 at a frequency of 70 cps between 5 seconds and the shutdown period. This vibration was not observed in the motion pictures. After the tip stabilizer had fully regripped the model, the pictures showed intermittent torsional vibration modes of first 124 cps and then, immediately preceding the shutdown disturbances, 70 cps; the 70-cps vibration was barely evidenced by strain gages 2 and 4. However, for the period between 11.6 seconds and 12.6 seconds, several frequencies could be obtained from the strain-gage traces; for instance, strain gage 13 showed a 275-cps frequency, strain gage 6 showed a 400-cps frequency, and strain gage 10 showed a 538-cps frequency. The small amplitudes and diversity of frequency suggest random excitation.

For times other than those during the starting, shutdown, and failure periods, all the noted vibrations were of small amplitude, probably resulting from the random noise and pressure disturbances in the vicinity

of the jet. Whenever the jet stagnation pressure was below 50 psi, which
was from the start until about 1.2 seconds and also from about 13.4 sec-
onds until complete shutdown of the jet, the model experienced violent
buffeting; when the stagnation pressure was between 50 and 100 psi, the
jet shock was passing over the model and creating random but much less
violent disturbances. The presence of the tip stabilizer in the air-
stream prior to the shutdown period evidently disturbed the flow in a
manner which excited the observed model torsional vibrations.

Temperatures

A typical temperature history of a skin and web is shown in figure 8
for a high-stagnation-temperature test. The temperature data from test
to test were compared by normalizing the data with respect to the test
conditions experienced by model MW-18 during test 1. The normalized tem-
perature was determined from the formula

$$T_b{}^* = \frac{\left(T_t - T_o\right)_a}{\left(T_t - T_o\right)_b}\left(T - T_o\right)_b + T_{o,a}$$

where the subscript a refers to the test conditions which existed during
the first test of model MW-18, and the subscript b refers to the test
conditions or model temperatures for the particular model under considera-
tion. The normalized temperatures plotted in figures 9 and 10 show that
the agreement among the model-temperature data was very good. Figure 9 is
a plot of the skin temperatures (midway between webs where the sink effect
of the web is negligible) that existed at 6 seconds test time. In general,
the skin temperatures decreased spanwise from the tip to the root and
chordwise from the leading edge to the trailing edge. A temperature dis-
tribution was calculated by the method outlined in reference 4 using the
Van Dreist method for calculating the heat-transfer coefficient; tunnel-
survey data were used to determine the adiabatic-wall temperature. It can
be seen from figures 9(b), 9(c), and 9(d) that the spanwise distribution
indicated in figure 9(a) is typical of each chord station. The spanwise
temperature variation is attributed to the parabolic-like stagnation-
temperature distribution that is a characteristic of the jet. The calcu-
lated line shown with the test data in figure 9(a) actually follows the
measured variation in the jet stagnation temperature.

Figure 10 shows the difference in the normalized temperatures between
the skin thermocouples and the web thermocouples for webs 3 and 4 at
specific span stations. This difference generally increases spanwise
because of the more rapid heating of the model at stations near the center
of the jet stream. However, significant deviations from this general

distribution may be taken as a rough indication of the local joint con-
ductivity. Figure 10 shows that, near the tip of model MW-18, the joint
conductivity was considerably below average for web 3, but was above
average for web 4.

Stresses

Experimental stresses.- Inasmuch as the state of stress in the model
skins was two-dimensional, stresses were determined from measured strains
only at points where two perpendicular gages were mounted. In order to
obtain the stresses at a given point, the chordwise and spanwise gages
were considered as being superimposed upon each other at the location of
the thermocouple placed between them. (See fig. 3(d).)

Several methods were tried in an attempt to account for temperature
effects on the strain data obtained from the strain gages. Although no
one method could be shown to lead to reliable and accurate strain data,
especially in the temperature range above 250° F, inspection of the results
indicated that the strain error could be as much as ±200 microinches per
inch. This would cause a skin-stress error of about ±2,000 to 3,000 psi,
which is of the same order of magnitude as the experimental stresses.

A survey of the strain data was made by using the measured values of
strain at 6 seconds test time. These data indicate that at the model root
the experimental chordwise strains were as much as twice the spanwise
strains. The gages mounted on opposite skins in the center bay near the
root indicate bending strains - counterclockwise strains (looking upstream)
for models MW-17 and MW-18 and clockwise strains for model MW-4-(2); only
one skin was instrumented at this point on model MW-16. The strain gages
indicated tensile stresses in the ribs and webs (except in the tip rib in
model MW-18 during the first test) for all the elevated-temperature tests.
During the cold-temperature test on model MW-16, the rib strains were com-
pressive; the conditions during this test were such that the model was
cooled. Compared with the web strains, the rib strains were small, with a
maximum rib strain (at 6 seconds) of 208 microinches per inch of tension
on the middle rib of model MW-18 during the first test. This condition
suggests that these ribs did not restrain the model skins as much in the
chordwise direction as the webs did in the spanwise direction; this may be
primarily due to the discontinuous nature of the ribs. The webs ran con-
tinuously over the span.

The strains measured on web 3 during the elevated-temperature tests
on models MW-16, MW-17, and MW-18 were in the same range (822 to 953 micro-
inches per inch of tension) at 6 seconds test time; whereas for the
elevated-temperature test on model MW-4-(2), the strain at this point was
1,280 microinches per inch of tension.

At the time considered (6 seconds test time) the model skin temperatures were such that, because of imperfect strain-gage temperature compensation, the range of error in the indicated strains could be as much as ±100 microinches per inch.

Calculated stresses.- The nonuniform temperature distribution over the models during high-stagnation-temperature tests gave rise to thermal stresses. Appendix E in reference 8 presents an approximate method for calculating these thermal stresses. This method, which does not take into account any influence on spanwise stresses caused by chordwise stresses, was used to calculate spanwise stresses at a cross section 3 inches from the tip of model MW-18, a section not influenced appreciably by chordwise ribs. At this section the general spanwise gradient was very small and was neglected. The experimental model temperatures (from test 1 of model MW-18) were used to determine the temperatures of the area elements shown in the idealized cross section in figure 11. Aerodynamic loads were neglected because it was assumed that, at zero angle of attack, only the drag force would appreciably add to the thermal stresses; preliminary calculations indicated that stresses due to drag load were less than 5 psi. End effects were also considered negligible at this section.

Figure 12 shows calculated skin stresses at the midchord and web stresses at the web center for the two webs immediately adjacent to the midchord (webs 3 and 4). The largest peak web stress (≈14,000 psi) was found to exist in web 3 and was a direct result of the low temperature measured at this point. This stress is 75 percent higher than the stress in web 4 and shows that for these test conditions the joint conductivity can have an important effect on the stresses. (See ref. 9.) Peak stresses for the other webs at the same spanwise station were between 8,000 and 10,000 psi with the 8,000-psi stress occurring in web 4. A somewhat above average value of joint conductivity is indicated in figure 10(b).

The skin stress histories at the bay centers were all similar, with peak stresses of about -3,000 psi. The maximum leading-edge stress, which occurred at 6 seconds test time, was calculated to be 740 psi; the maximum trailing-edge stress of 1,750 psi occurred at 9 seconds.

Comparison of calculated and experimental stresses.- Several significant facts are apparent from a comparison of the calculated stresses with the experimental-stress values obtained from the strain data for model MW-18. Both the experimental and calculated spanwise skin stresses have a magnitude of about -3,000 psi at the section 3 inches from the model tip. The strain gages also show that the chordwise stresses at this section were about 2,000 psi. This value of chordwise strain, considered with the low values of rib stress and small rib area (when compared with the skin area on a spanwise section), indicates that

some form of chordwise restraint, other than the ribs, was present. Such a restraint exists in a flat plate which is clamped at one edge and is subjected to a uniform temperature rise. (See ref. 10.) Calculations using the methods outlined in this reference indicate that the root restraint will induce chordwise stresses in the same range as those measured at a distance 3 inches from the tip of model MW-18.

The singularly high calculated peak stress in web 3 in model MW-18 is a direct consequence of the relatively low temperature measured at this location and probably results from a low, local joint conductivity which retarded the heat flow into the web. The joint conductivity may be expected to vary from one location to another, inasmuch as it is a function of such things as tightness of joint and contact-surface condition of materials (things which are difficult to evaluate on other than a statistical basis).

The low values of strain (when considered with the ratio of rib area to skin area) measured in the ribs show that the assumption that chordwise rib restraint could be neglected in the spanwise stress calculations was valid for these model tests. Inasmuch as the strain gages on the chordwise ribs in models MW-16, MW-17, and MW-18 indicated that these members contributed little thermal-stress restraint to the models, the stress calculations at the section 3 inches from the tip on model MW-18 should also apply to all the other models in this group provided the stresses are normalized with respect to the individual test conditions (with respect to the difference between the test stagnation temperature and the initial temperature of the model).

Discussion of Failure

The first test of model MW-4-(2), which occurred under conditions where aerodynamic heating was not present, showed that, although this design may be near-marginal, the model was strong enough to withstand the aerodynamic forces at a Mach number of 2 and sea-level static pressure and was stiff enough to resist flutter under these test conditions. The second test, made at a stagnation temperature of 563° F, added thermal stresses due to aerodynamic heating to the stresses caused by aerodynamic loading and reduced the modulus of elasticity of the aluminum alloy. Both the thermal stress and the reduced modulus contributed to the decrease of the effective stiffness of the model; a chordwise flutter mode developed, and the model completely destroyed 0.36 second after the flutter mode began. The first model (model MW-4) of this design had been previously tested and had failed at 5.60 seconds after the start of the test (ref. 4); whereas model MW-4-(2) failed at 7.68 seconds after the start of the test. Other than the small difference in the time of failure, the two models failed in a very similar manner: both failed 0.36 second after the

beginning of the flutter mode; the flutter frequency of model MW-4 was 240 cps and that of model MW-4-(2) was 238 cps; and both models failed when the large distortions of the cross section crushed the tip rib.

A comparison of the test conditions of the two models shows that the thermal stresses in model MW-4 should be about 10 percent lower than those in model MW-4-(2) (see appendix of ref. 3); however, a comparison of the normalized temperature distributions between the two models leads to discrepancies which indicate that the methods used to determine aerodynamic test conditions did not give compatible values between the two sets of tests. In reference 4 two probes mounted on posts behind the model were used to measure the stagnation temperatures; whereas for the tests reported herein, probes mounted in the screen section just downstream from the jet settling chamber were used either exclusively or were averaged with the probes mounted behind the model. As a check, the experimental adiabatic-wall temperature was calculated for model MW-18 in run 1 by using the model temperature data (see ref. 4), and the stagnation temperature was then calculated by using a recovery factor of 0.88. The resulting stagnation temperature, as experienced by the model, was 480° F, which was considerably lower than the stagnation temperature of 523° F indicated by the tunnel data. The results, if the data agreement in figure 9 is used as justification, may be extrapolated to the elevated-temperature test on MW-4-(2). The temperature comparison indicates that, if the stagnation temperature in the test on MW-4-(2) had been lower, better agreement would be found among the test data between the MW-4 design models; this would also have the effect of lowering the stress level in model MW-4-(2) to that in model MW-4. Thus, the small discrepancy in time of failure between the two models can be partly attributed to experimental error in determining the test conditions. A difference in joint conductivity between the two models also might have influenced the time of failure, but no reliable comparison between the models could be made since the only skin-and-web thermocouple combination available in model MW-4-(2) was near the root, a position where the parabolic-like stagnation-temperature profile across the jet stream would cause the temperature difference between these somewhat offset (spanwise) thermocouples to be questionable. (See fig. 3(a).)

Studies of a cross section of the MW-4 design show that the mode of cross-sectional distortion observed during the flutter of models MW-4 and MW-4-(2) may be induced by applying shearing loads to the skins in such a manner that the opposite skins tend to slide with respect to each other. (The same effect may be obtained by applying equal moments and equal and opposite forces at the leading and trailing edges, respectively.) If the riveted joints between the webs and the skins are replaced by pinned connections, the cross section in figure 1(a) becomes a series of four-bar linkages and will have no resistance to distortion; also, if the aforementioned loading is applied, the cross section will distort into a shape

approximating the distortion of the cross section during flutter. This shape is a direct result of the fact that the opposite skins are not parallel to each other (except at the center chord) but instead slope together. In the actual model, however, the skin is continuous and must bend when the cross section distorts; for ribless models, then, the skin bending stiffness is a criterion in determining the flutter resistance.

The major effect of the chordwise ribs in models MW-16, MW-17, and MW-18 was not to increase the skin bending stiffness but to restrain the chordwise distortion by preventing the skins from sliding past each other at points other than those at the leading and trailing edges. It may be possible to add sufficient restraint (for these test conditions) by using only a partial chordwise rib extending over one or two cells; if one or two cells are restrained, the effective stiffness of the entire cross section against this type of distortion is increased.

SUMMARY OF RESULTS

Four multiweb wing models of 20-inch chord and span with 0.064-inch-thick skin, 0.025-inch-thick ribs and webs, and zero, one, two, or three chordwise ribs were tested. The following results are given:

1. The model without chordwise ribs survived the first test where aerodynamic-heating effects were absent, but it failed during the second test when heating effects were included; thus, the present test confirmed the conclusions formed after an earlier test on another model of the same design (see NACA Research Memorandum L57H01) that aerodynamic heating made the model susceptible to flutter.

2. The mode of flutter failure involved distortion of the entire cross section of the model, a condition which required that the individual cells of the model cross section distort and the opposite skins slide with respect to each other. Chordwise ribs helped to restrain this sliding tendency. One chordwise rib was sufficient to prevent flutter of this model design under these test conditions. The addition of one chordwise rib nearly doubled the lowest natural frequency at which chordwise deformation occurred.

3. The temperature data compared very well from model to model on a normalized basis.

4. The experimentally measured stresses were well below yield stresses for the aluminum alloy used in the model construction. The largest stresses were in the spanwise webs. Chordwise skin stresses near the model roots were larger than those elsewhere in the skin because of the

large restraint at this location. Direct rib stresses were small. The
error in the measured strains is estimated to be about the same as the
skin strains caused by thermal stresses.
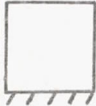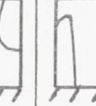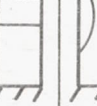
5. The thermal stresses calculated for one model were in agreement
with the measured stresses within the accuracy of the test data. The
low strains measured in the chordwise ribs indicate that these calcula-
tions which neglect the restraint of ribs may be extrapolated to the
other models with more or fewer ribs.

Langley Aeronautical Laboratory,
    National Advisory Committee for Aeronautics,
        Langley Field, Va., November 27, 1957.

REFERENCES

1. Heldenfels, Richard R., Rosecrans, Richard, and Griffith, George E.:
   Test of an Aerodynamically Heated Multiweb Wing Structure (MW-1)
   in a Free Jet at Mach Number 2. NACA RM L53E27, 1953.

2. Griffith, George E., Miltonberger, Georgene H., and Rosecrans, Richard:
   Tests of Aerodynamically Heated Multiweb Wing Structures in a Free Jet
   at Mach Number 2 - Two Aluminum-Alloy Models of 20-Inch Chord With
   0.064- and 0.081-Inch-Thick Skin. NACA RM L55F13, 1955.

3. Heldenfels Richard R., and Rosecrans, Richard: Preliminary Results of
   Supersonic-Jet Tests of Simplified Wing Structures. NACA RM L53E26a,
   1953.

4. Rosecrans, Richard, Vosteen, Louis F., and Batdorf, William J., Jr.:
   Tests of Aerodynamically Heated Multiweb Wing Structures in a Free
   Jet at Mach Number 2 - Three Aluminum-Alloy Models and One Steel
   Model of 20-Inch Chord and Span With Various Internal Structures
   and Skin Thicknesses. NACA RM L57H01, 1957.

5. Miltonberger, Georgene H., Griffith, George E., and Davidson, John R.:
   Tests of Aerodynamically Heated Multiweb Wing Structures in a Free
   Jet at Mach Number 2 - Two Aluminum-Alloy Models of 20-Inch Chord
   With 0.064-Inch-Thick Skin at Angles of Attack of 0° and ±2°. NACA
   RM L57H19, 1957.

6. Vosteen, Louis F., and Fuller, Kenneth E.: Behavior of a Cantilever
   Plate Under Rapid-Heating Conditions. NACA RM L55E20c, 1955.

7. Vosteen, Louis F., McWithey, Robert R., and Thompson, Robert G.:
   Effect of Transient Heating on Vibration Frequencies of Some Simple
   Wing Structures. NACA TN 4054, 1957.

8. Heldenfels, Richard R.: The Effect of Nonuniform Temperature Distri-
   butions on the Stresses and Distortions of Stiffened-Shell Structures.
   NACA TN 2240, 1950.

9. Griffith, George E., and Miltonberger, Georgene H.: Some Effects of
   Joint Conductivity on the Temperatures and Thermal Stresses in Aero-
   dynamically Heated Skin-Stiffener Combinations. NACA TN 3699, 1956.

10. Aleck, B. J.: Thermal Stresses in a Rectangular Plate Clamped Along
    an Edge. Jour. Appl. Mech., vol. 16, no. 2, June 1949, pp. 118-122.

TABLE I.- NATURAL VIBRATION MODES AND FREQUENCIES FOR MODELS

Model	Frequency, cps, for node line[a] -										
	A	B	C	D	E	F	G	H	I	J	K
MW-4-(2)	72	144	268	---	392	---	427	---	529	---	---
MW-18	73	156	---	326	---	465	---	---	---	---	585
MW-17	75	160	---	335	---	533	---	---	---	746	661
MW-16	70	147	---	318	---	554	---	439	---	747	677

[a]Modes shown are composites from modes for all models. Individual modes varied slightly from those shown. Sketches show node lines obtained during room-temperature vibration tests.

TABLE II.- AERODYNAMIC-TEST-DATA SUMMARY GIVING AVERAGED TEST CONDITIONS

Model	Test	Stagnation pressure, psia	Stagnation temperature, °F	Free-stream static pressure, psia	Free-stream dynamic pressure, psi	Free-stream temperature, °F	Free-stream velocity, fps	Free-stream density, slugs/cu ft	Speed of sound, fps	Reynolds number per foot
MW-4-(2)	1	110	93	14.3	39.8	-152	1,713	3.90×10^{-3}	861	27.7×10^{6}
	2	116	563	15.1	41.7	111	2,330	2.21	1,171	12.8
MW-16	1	114	111	14.8	41.0	-141	1,741	3.89	875	26.1
	2	116	521	15.1	41.8	89	2,284	2.30	1,148	13.4
	3	115	514	15.0	41.5	84	2,275	2.31	1,143	13.5
	4	112	506	14.5	40.2	79	2,265	2.26	1,138	13.3
MW-17	1	114	530	14.8	41.2	92	2,292	2.26	1,152	13.2
	2	113	524	14.7	40.7	89	2,284	2.39	1,148	13.9
MW-18	1	114	523	14.9	41.0	88	2,285	2.26	1,148	13.3
	2	114	556	14.8	41.0	107	2,322	2.19	1,167	12.6

TABLE III.- MODEL TEMPERATURE HISTORIES

Model	Test	t, sec	1	2	3	4	5	6	7	8	9	10	11	12	13	14	15	16	17	18	19	20	21	22	23	24	25	26	27	28	29	30
MW-4-(2)	1	0		74		80	79	80	78	77	81	81	79	79	78	78	79	79	83	84	82	83	81	82	77	82	81	82	88		81	
		1		75		84	83	83	79	77	84	86	83	82	81	81	78	78	84	86	84	85	84	82	78	79	84	85	91		88	
		2		80		88	88	86	82	78	84	88	85	82	82	80	79	80	88	90	88	87	84	84	80	79	85	87	91		82	
		3		80		84	88	87	85	82	83	81	85	85	83	83	80	81	81	87	86	87	87	82	82	80	79	81	84	88		79	
		4		83		83	84	83	83	83	82	85	82	83	83	83	81	81	86	83	83	86	79	77	79	81	78	85	83	88		81	
		5		83		81	84	84	83	83	82	85	82	83	83	84	80	79	84	81	82	85	76	78	82	78	83	83	87		83	
		6		83		80	84	83	83	84	83	85	82	82	82	81	82	81	78	83	81	80	83	74	77	81	79	83	81	84		80	
		7		82		79	83	83	82	82	83	84	82	82	81	80	82	82	78	83	79	81	82	74	75	81	80	83	80	85		80	
		8		82		79	82	83	83	82	82	83	81	80	80	82	82	81	77	83	79	81	82	74	75	81	81	81	78	82		80	
		9		82		79	81	82	81	80	81	82	81	81	80	81	81	81	77	83	80	79	82	73	75	81	81	82	78	82		76	
		10		81		77	82	82	81	80	81	81	80	79	80	80	82	76	83	79	79	80	72	74	79	80	79	78	83		80	
		11		81		76	81	81	81	81	82	79	79	79	80	82	75	83	78	79	81	71	75	80	79	81	83	78	82		80	
		12		81		77	80	80	81	79	81	80	79	79	80	81	80	73	81	77	78	80	71	70	79	81	79	78	82		80	
		13		81		77	80	80	79	80	80	78	79	79	81	81	81	74	81	78	78	80	69	70	79	81	83	78	83		82	
		14		79		75	80	79	79	81	81	79	79	78	79	81	80	74	83	77	77	81	68	69	79	85	79	78	82		85	
		15		79		75	81	81	80	79	82	81	79	79	81	81	72	82	77	77	81	70	71	78	83	79	78	82		81	
	2	0	80	79		86	83	82		78	81	82	83	79	80		81	80	82	86	79		80	75				84	85			79	
		1	104	93		122		129	95	82	127	126	118	95	97		79	81	124	123	118		112	108				116	118			94	
		2	178	141		188		193	135	95	191	193	174	134	135		75	90	182	193	187		165	156				183	191			141	
		3	256	205		249		254	190	133	250	254	230	181	182	113	109	237	250	244		211	200				226	240			178	
		4	317	263		293		300	239	180	293	301	271	231	226		138	282	294	287		245	235				261	280			210	
		5	364	314		327		337	282	226	331	336	307	268	265		169	316	329	322		271	260				289	311			239	
		6	396	355		351		366	320	271	361	366	336	301	299		198	345	358	350		292	283				313	338			265	
		7	419	389		371		390	351	308	385	389	362	331	320		227	369	381	374		308	300				335	362			288	
MW-16	1	0	83	82	88	84	85		90	87		82	82	88	82	87	84	85	88	89	86	83	83	88	87		87	85	85	85	85		
		1	85	84	93	90	87		95	93		83	84	92	86	89	87	85	92	95	87	84	79	91	89		90	86	86	86	88		
		2	90	87	95	90	89		97	95		84	83	95	90	91	87	86	96	96	89	85	78	93	92		94	88	89	90	92		
		3	92	89	96	94	89		97	95		86	85	94	90	88	86	87	94	92	90	87	79	93	91		93	89	90	90	91		
		4	92	90	94	93	87		95	94		87	85	92	89	86	84	88	93	89	91	88	79	92	90		91	89	89	89	90		
		5	92	91	93	92	84		94	94		87	85	91	88	85	83	88	92	87	91	87	79	91	89		91	89	89	89	88		
		6	92	91	93	91	84		94	92		88	84	90	87	83	82	87	91	86	91	87	80	89	89		89	88	88	88	88		
		7	92	90	93	91	83		94	93		87	84	89	86	82	81	87	91	86	91	87	79	89	87		90	87	88	88	88		
		8	91	90	93	91	83		93	91		88	84	88	86	82	80	86	90	85	90	87	79	88	85		89	86	88	87	87		
		9	91	90	91	90	82		92	91		87	83	88	85	80	79	84	89	85	90	86	78	88	86		89	85	87	86	87		
		10	90	89	91	90	82		92	90		87	82	87	85	80	78	83	88	83	89	85	79	87	86		89	86	87	86	88		
		11	90	90	91	89	81		91	90		86	81	86	84	80	78	82	88	83	88	85	79	87	86		89	86	88	88	88		
		12	90	89	91	88	81		90	89		86	81	86	84	79	75	82	88	83	88	85	79	87	86		88	86	87	87	87		
		13	89	89	91	87	80		90	92		87	84	87	84	79	73	81	88	83	89	86	79	87	86		88	86	87	87	87		
		14	88	88	90	88	80		90	94		86	81	86	83	78	75	81	88	82	90	85	87	85	84		88	86	87	87	87		
		15	88	88	89	88	80		90	92		86	80	87	83	78	76	80	89	83	88	85	86	85	86		87	86	87	86	87		
	2	0		82	81	85	83	82	82	86		78	82		77	83	79	83	81	80	85	83	81	78			84		83	81	80	81	81
		1		106	91	126	130	101	85	127		82	79		82	121	116	103	102	82	115	153	84	81			114		109	88	87	93	105
		2		171	128	183	202	139	108	192		93	145		85	185	180	143	143	89	171	238	95	93			171		160	113	117	135	162
		3		239	180	245	265	185	153	253		117	191		102	238	233	183	186	107	219	289	121	115			210		194	143	148	168	197
		4		293	229	293	312	220	202	298		150	232		125	279	273	214	218	129	256	324	148	143			244		220	170	176	197	225
		5		334	273	331	346	248	248	333		184	264		151	311	307	237	244	154	287	349	178	173			272		248	196	203	224	251
		6		364	309	357	371	269	280	360		219	290		177	337	333	256	263	178	311	369	202	202			292		267	216	227	244	273
		7		387	338	380	388	284	317	380		249	316		200	358	354	271	278	201	331	384	229	228			316		288	240	250	267	294
		8		405	363	396	402	297	343	396		276	336		222	374	371	283	292	222	349	396	252	252			334		307	259	269	287	311
		9		417	382	409	412	307	363	408		300	352		242	387	385	298	301		361	405	273	275			350		324	277	287	305	329
		10		427	397	419	419	315	379	418		321	364		259	398	391	300	309		372	414	291	293			363		337	293	305	321	343
		11		435	410	427	425	321	392	424		339	376		274	407	406	307	315		381	419	308	311			373		351	308	319	335	354
		12		440	419	433	428	327	409	430		350	387		284	413	412	311	320		388	425	321	325			382		363	323	334	350	367
		13		445	426	439	430	331	410	434		364	394		295	417	419	314	309		393	432	337	340			396		380	341	352	367	384
		14		447	431	435	434	325	417	427		375	—		—	409	413	311	309		396	403	352	353			389		383	354	364	375	386
		15		447	434	432	432	327	421	427		376	406		297	406	410	308	305		393	403	361	362			386		381	360	368	377	384
		16		447	435	431	431	326	423	425		378	408		302	404	408	306	304		393	404	368	367			384		381	363	370	377	382
	3	0		74	72	77	76	74	72	76		76	76		72	73	72	75	74	71	76	77	72	70			74		72		73	72	72
		1		95	82	109	120	96	76	111		75	79		70	107	103	101	101	75	107	134	75	74			103		100		78	85	94
		2		151	116	156	186	142	96	167		138	86		81	180	173	142	138	82	168	220	85	86			165		144		107	124	144
		3		215	165	214	244	182	139	220		181	110		99	231	220	178	177	100	214	266	108	107			204		174		138	156	178
		4		265	211	259	287	213	185	263		215	141		121	270	260	205	206	122	250	297	135	131			238		200		166	183	205
		5		304	249	295	319	235	229	299		247	173		146	301	287	226	228	146	278	318	164	159			266		224		193	209	229
		6		342	288	324	343	256	265	327		273	207		172	327	315	246	249	169	303	338	191	187			289		245		217	233	252
		7		358	318	347	363	271	298	352		296	239		196	348	336	262	264	189	324	353	216	213			309		264		238	253	270
		8		377	340	366	377	282	323	371		316	265		219	364	354	273	276	210	341	365	239	237			327		281		259	273	287
		9		392	360	380	389	292	344	386		333	289		238	378	368	282	285	228	354	374	260	259			341		297		277	289	302
		10		403	375	392	398	299	360	397		346	313		256	390	380	290	293	244	366	382	278	278			355		312		293	304	316
		11		412	389	400	404	304	373	405		357	327		270	397	390	296	299	258	374	388	296	293			367		324		308	318	328
		12		419	396	407	410	309	382	414		369	343		282	405	398	300	303	272	382	391	311	310			378		336		320	332	341
		13		422	405	413	413	312	390	415		376	354		291	410	403	303	298	282	389	397	323	324			390		351		336	348	358
		14		425	411	422	417	307	398	417			364		292	415	411	301	292	289	400	390	339	341			393		361		352	361	367
		15		425	415	415	417	307	402	408		391	370		319	406	401	299	292	296	398	378	349	348			385		357		356	363	366
	4	0		85	84	88	87	82		89		88	84		81	90	84	84	79	81	87	85	86	84			86		85	84	82	84	85
		1		109	95	124	135	106		124		118	86		82	123	116	106	107	83	119	136	88	87			113		112	90	90	96	107
		2		167	130	157	197	148		175		148	93		87	183	178	144	143	90	170	223	100	96			169		157	115	117	134	161
		3		229	177	210	255	192		227		192	112		104	231	221	206	210	107	214	272	118	114			211		212	168	174	192	213
		4		277	221	253	298	222		273		230	138		122	272	263	206	210	127	251	304	143	138			267		234	192	202	215	241
		5		311	263	289	328	246		308		261	170		145	303	294	227	232	148	279	327	171	165			291		255	214	223	236	260
		6		342	296	317	353	264		335		289	202		170	331	319	243	250	168	305	344	196	190			310		274	233	244	255	278
		7		365	321	340	371	278		357		308	231		193	346	340	257	265	188	322	360	219	215			326		294	251	261	273	294
		8		382	346	357	385	287		377		327	258		214	362	357	268	275	206	337	371	242	237			341		307	268	277	289	308
		9		396	365	372	396	296		393		344	282		232	375	371	277	284	221	351	381	263	258			353		319	284	293	303	321
		10		407	380	385	405	304		403		356	303		247	387	381	283	291	236	361	389	280	275			364		331	297	307	316	331
		11		415	392	395	411	309		412		370	320		260	396	391	289	297	250	368	396	296	291			364		339	311	320	329	343
		12		420	401	404	415	313		418		376	333		267	401	394	292	296	262	377	402	309	305			376		346	311	320	345	359
		13		424	409	412	417	312		425		380	342		268	410	406	288	287	270	383	406	325	319			387		361	324	336	345	359
		14		424	411	411	419	306				387	351		270	401	394	288	276	284	384	390	331				377		352	336	343	349	360
		15		425	415	408	417	306				388	357		275	400	392	284	285	287	384	382	347	338			375		359	339	346	352	358

TABLE III.- MODEL TEMPERATURE HISTORIES - Concluded

Model	Test	t, sec	\ Temperature, °F, at thermocouple[a] -														**16**																		
			1	2	3	4	5	6	7	8	9	10	11	12	13	14	15	16	17	18	19	20	21	22	23	24	25	26	27	28	29	30	32	33	34	35
MW-17	1	0	70	71	68		68	66	68	68	68	66	60	69	66	68	68	69	72	68	71	72	69	69	68	64	64	65	68	71		69	69	70	68	70
		1	116	105	72		101	66	97	92	83	68	67	70	104	103	101	101	106	106	105	104	101	93	96	67	65	65	90	90		89	133	169	166	127
		2	195	160	88		150	75	144	130	118	82	78	78	173	171	173	170	167	171	166	158	162	132	137	75	77	73	131	113		117	167	209	206	159
		3	263	207	119		195	97	188	168	153	107	103	93	228	224	223	217	211	220	218	208	214	171	177	98	101	89	168	145		146	194	243	239	184
		4	309	241	156		228	124	219	197	183	139	134	116	269	265	259	254	248	257	259	246	252	198	208	123	131	112	196	181		176	217	270	265	204
		5	344	266	190		253	156	245	222	210	172	167	139	302	297	291	284	276	287	291	277	283	222	232	150	162	136	220	214		205	236	294	288	221
		6	371	284	219		271	185	265	243	232	203	200	162	329	316	309	301	311	318	302	309	240	251	177	193	159	238	242		230	251	315	309	234
		7	390	298	245		285	210	278	257	250	232	231	184	352	348	336	331	323	331	339	323	329	255	267	203	222	182	252	281		254	263	333	325	245
		8	404	310	261		295	231	290	270	266	259	257	203	370	365	353	346	341	348	356	340	345	267	279	227	248	200	265	293		274	274	350	342	255
		9	417	319	281		305	247	298	280	279	281	283	220	384	380	367	361	358	361	371	356	360	278	287	248	270	220	276	313		291	281	362	355	262
		10	426	324	294		313	260	306	291	290	300	305	235	395	391	379	375	369	374	384	367	369	286	269	292	235	283	329			308	289	374	367	267
		11	434	328	304		317	271	311	296	298	316	324	248	406	402	389	386	380	383	393	377	377	292	285	310	248	290	344			324	289	385	379	260
		12	437	331	311		320	281	314	301	305	330	335	257	412	409	397	392	388	389	395	404	390	386	296	303	320	338	268	288	369		341	281	398	390	257
		13	439	330	318		321	289	315	301	310	342		267	417	417	407	405	401	409	398	391		293	300	333	355	274	286	384		360	284	397	392	263
		14	433	324	321		315	295	310	299	313	352		274	417	417	417	407	405	401	409	398	391	293	300	355	274	286	384		367	283	394	387	263
		15	429	324	319		314	296	308	299	314	358		277	413	413	405	403	399	402	408	396	388	291	301	343	365	278	287	388						
MW-17	2	0	87	87	83		83	81	83	84	87	81		85	80	79	85	87	86	86	88	89	86	86	82	80	80	83	85	85	86		86	87	83	86
		1	136	118	87		114	81	113	109	104	83		86	118	117	118	122	120	123	122	122	120	109	108	85	83	84	109	100	108		109	119	115	107
		2	209	169	102		160	93	156	145	135	96		93	181	178	179	179	173	183	179	171	173	144	147	92	94	89	145	118	148		146	180	176	139
		3	272	212	131		200	112	195	178	165	119		109	232	229	226	224	215	227	226	215	219	178	183	106	117	104	179	141	185		176	217	214	168
		4	315	245	163		230	138	224	205	192	150		130	272	268	262	258	249	261	263	251	255	205	212	122	144	123	205	164	218		201	246	246	190
		5	348	267	193		254	163	246	227	217	182		150	305	300	291	287	278	290	294	280	284	224	235	142	174	145	227	189	248		222	276	272	208
		6	374	284	220		272	188	265	247	237	211		171	331	326	316	311	302	319	319	304	307	244	254	164	202	166	243	216	274		239	298	295	223
		7	393	296	242		285	212	280	261	256	239		191	352	347	336	331	322	334	339	323	327	259	269	189	230	187	257	255	297		253	317	314	234
		8	407	307	260		296	231	291	273	271	264		208	369	365	353	349	342	343	349	342	343	272	280	211	254	208	270	285	317		266	334	331	246
		9	419	317	276		304	248	300	284	284	286		224	384	379	367	364	355	363	371	355	355	281	291	232	277	224	278	305	334		275	350	347	255
		10	429	323	289		311	261	307	291	295	304		237	396	391	379	377	374	382	386	366	377	295	304	271	314	253	292	336	362		289	373	372	265
		11	435	327	300		316	273	312	297	303	321		248	405	402	388	385	377	382	391	377	374	300	307	289	328	265	285	353	376		285	387	383	257
		12	439	330	308		319	282	316	302	309	334		259	411	408	395	392	385	390	398	384	379	300	307	300	344	273	292	365	384		285	399	396	263
		13	440	331	315		319	290	314	302	314	346		268	422	418			403	402	395	400	403	390	295	300	307	327	359	276	290	383	391		286	393	386
		14	433	325	317		316	295	312	301	317	356		271	414	413			406	402	395	400	407	397	385	294	302	327	359	276	290	383	391		284	391	386	264
		15	431	324	318		315	297	310	299	317	361		277	412			403	402	395	400	405	384	381	290	322	365	281	290	385	386						
MW-18	1	0	83	77		78			79	82	84		80	81	77	78	80					84	79	82	82	78	77	78	79	81	83	82	82	83	79	
		1	126	111		81			117	122	121		110	105	84	82	80	78	114			120	118	84	117	118	104	103	90	81	117	102	86	113	116	105
		2	201	164		95			189	186	183		157	159	88	95	91	87	182			180	190	175	137	182	146	160	128	104	228	184	129	212	222	176
		3	266	210		125			248	243	238		201	205	98	119	120	103	234			230	231	103	226	224	184	181	139	104	228	184	129	212	222	176
		4	313	243		163			290	282	281		234	244	118	153	155	128	275			269	270	122	264	260	211	173	125	266	224	160	245	255	199	
		5	348	268		202			326	316	314		261	278	142	187	194	153	304			300	302	143	293	292	238	237	212	150	300	256	191	272	282	219
		6	376	286		239			352	342	340		281	308	170	230	179		329			326	328	167	317	317	257	256	284	220	297	305	236			
		7	397	300		272			373	362	363		297	334	198	251	262	202	350			347	348	192	336	338	271	273	284	196	348	310	247	317	326	250
		8	412	310		303			391	380	382		311	357	224	278	291	218	367			363	364	217	355	355	285	285	293	216	367	335	345	351	360	261
		9	425	319		328			405	394	395		321	376	249	304	318	242	383			377	377	240	370	368	294	297	319	235	382	345	290	351	360	271
		10	436	325		350			416	405	406		329	390	273	324	339	257	395			388	390	260	382	379	302	305	344	252	395	357	310	364	372	279
		11	444	333		368			426	413	415		336	403	297	342	357	271	404			398	398	281	387	387	308	315	368	267	406	368	328	375	384	289
		12	449	335		384			431	418	421		339	412	312	356	371	282	412			402	404	299	398	392	312	316	375	278	415	380	342	387	396	289
		13		335		397			435	422	424		337	419	324	367	383	291	422			407	412	335	404	401	307	310	396	295	396	371	354	397	402	293
		14		332		405				420	427		335	420	348	382	374	293	417			410	412	335	413	401	307	310	396	295	398	377	394	401	290	
		15		329		401				420	425		333	421	360	391	370	300	414			410	410	333	413	396	305	309	398	301						
MW-18	2	0	78			74	73		77	79	74		74			76	73		76			76		76	78	74				79		72	74	75	72	79
		1	113			80	77		120	118	119	111	98		77	77	112		116			117	113	107	103					79		89	78	102	108	107
		2	174			89	92		186	186	182	164	155		92	84	188		185			184	172	146	142	108				86		109	96	168	182	151
		3	226			101	126		246	248	241	213	204		118	102	245		243			242	229	198	192					98		140	124	210	226	185
		4	261			128	168		291	294	285	251	248		154	126	288		286			270	262	239	225					117		175	158	247	262	212
		5	286			161	210		328	331	321	279	285		192	153	320		320			321	305	256	253					141		211	190	279	293	234
		6	307			195	250		357	361	349	302	318		229	180	347		347			350	333	278	275					165		245	220	304	318	251
		7	324			228	283		378	385	371	321	346		262	206	367		369			372	356	294	294					190		275	250	327	341	266
		8	334			258	311		397	405	389	334	371		291	230	387		386			393	375	307	307					214		302	275	345	359	280
		9	345			284	339		412	419	401	347	390		320	251	405		402			406	389	319	330					234		326	298	366	375	291
		10	352			307	360		425	431	413	356	406		341	267	415		413			418	403	327	330					253		348	319	378	390	300
		11	357			329	379		436	441	422	362	420		361	284	424		421			428	411	334	334					271		365	337	390	401	307
		12	361			352	393		440	446	427	368	430		377	296	433		427			432	414	338	340					285		382	354	402	411	311
		13	364			389	409		443	449	429	370	441		392	309	443		432			437	419	334	333					300		400	370	417	428	312
		14	358			410	416			453	433	363	447		405	317	444		436			441	425	334	333					309		416		420	426	315
		15	357			408	422			451	433	362	444		410	323	439		434			441	420	333	333					314		422		415	423	314

[a] Blanks in data denote that the instrument was not used.

TABLE IV.- MODEL STRAIN HISTORIES

Model	Test	t, sec	Strain, microinches per inch, at strain gage location[a]																		
			1	2	3	4	5	6	7	8	9	10	11	12	13	14	15	16	17	18	19
MW-4-(2)	1	0		4				-7	2	-8	-36	2	8	15	-4	2			-4		
		1		-91				-32	62	-57	36	-255	49	-36	-58	-51			13		
		2		-95				-10	-99	63	-100	-25	-259	34	-93	-103			-57		
		3		-8				-7	-45	49	-34	-54	-206	-23	-25	-125			-2		
		4		44				0	-54	61	-24	-45	-213	-61	-24	-133			0		
		5		65				5	-56	73	0	-45	-206	-63	-18	----			13		
		6		44				2	-73	61	2	-50	-212	-80	-29	----			-2		
		7		65				0	-77	71	17	-52	-219	-79	-36	----			-2		
		8		46				0	-86	71	19	-58	-223	-77	-31	----			4		
		9		17				7	-101	69	15	-56	-244	-73	-49	----			8		
		10		-21				17	-170	131	-32	37	-336	-63	-84	----			-42		
		11		-110				2	-198	113	-24	-27	-261	-40	-73	----			-8		
		12		-237				8	144	26	86	-195	-36	-138	-44	----			-4		
		13		-17				27	-54	105	73	-52	-166	-71	-73	----			-46		
		14		42				---	-172	---	19	402	-623	-33	---	----			4		
		15		17				---	-21	---	141	-174	-162	-65	---	----			-4		
	2	0		4	17		17				-22	12	8								
		1		388	360		103				-160	222	-55								
		2		297	930		238				-462	330	-6								
		3		212	1285		215				-701	290	-29								
		4		115	1393		145				-908	199	-129								
		5		87	1374		131				-1058	143	-230								
		6		84	1283		131				-1069	75	-273								
		7		72	1140		189				-994	14	-298								
MW-16	1	0	13	0	-17	4		23		-4	-2			-6	4	8	2	4	0		
		1	73	-40	75	35		90		0	68			0	24	17	-64	-125	7		
		2	105	-96	93	6		75		40	77			-8	-49	-9	-185	-63	-154		
		3	202	-42	155	57		81		-19	124			27	-77	-11	-123	-87	-145		
		4	192	-42	159	64		49		-15	122			-8	-88	-19	-163	-79	-139		
		5	170	-4	168	62		36		4	112			41	-82	-24	-167	-161	-177		
		6	164	23	170	66		32		15	114			27	-97	-32	-229	-146	-225		
		7	143	2	155	39		21		11	105			33	-84	-26	-209	-146	-226		
		8	119	19	155	31		19		34	99			23	-82	-23	-253	-179	-237		
		9	96	12	141	37		6		61	110			33	-60	-24	-161	-88	-139		
		10	55	23	122	37		-15		91	170			263	-101	-43	-159	-102	-170		
		11	2	-19	52	21		-34		67	143			421	-110	23	-169	-56	-188		
		12	-66	-35	-14	-90		45		36	-46			270	339	86	-112	15	-132		
		13	26	-29	56	27		9		17	149			-2	15	-11	-237	-92	-91		
		14	23	27	97	-92		58		0	165			---	5	---	-127	10	-4		
		15	40	36	83	-21		69		10	29			---	9	---	-119	2	5		
	2	0				2		22		19	6						2		0	4	
		1				13		327		68	63						32		122	210	
		2				130		760		236	201						107		-7	44	
		3				70		1026		243	137						151		-46	-2	
		4				50		1085		239	33						155		-122	-12	
		5				57		1039		192	-90						135		-161	-6	
		6				48		944		177	-153						111		-135	-13	
		7				29		805		287	-185						62		-89	0	
		8				32		651		363	-161						24		-68	2	
		9				48		487		365	-133						-66		-41	54	
		10				57		320		298	-94						-177		-54	110	
		11				95		147		239	-46						-232		-35	158	
		12				78		-15		226	59						-228		307	416	
		13				63		-91		625	-76						-161		96	325	
		14				-30		-121		---	-222						-139		----	---	
		15				99		-217		---	13						-226		----	---	
		16				107		-279		---	24						-254		----	---	
	3	0				-9		21			-4						2	5			9
		1				44		300			96						34	24			62
		2				87		709			101						153	102			83
		3				47		914			62						194	138			64
		4				59		968			42						195	145			26
		5				87		932			5						189	133			0
		6				118		845			-16						168	112			-40
		7				117		727			-52						140	73			-26
		8				120		614			-56						116	22			-23
		9				130		477			-47						94	-10			-32
		10				134		348			-40						80	-37			-36
		11				125		216			-51						76	-66			17
		12				122		102			-54						83	-87			11
		13				70		-18			-14						172	43			162
		14				132		-43			-63						236	-31			19
		15				104		-131			-83						166	-61			75
	4	0				-14		9			-5						46	-4			
		1				83		261			113						144	-5			
		2				31		683			57						141	72			
		3				17		895			19						188	116			
		4				36		948			-14						207	125			
		5				61		902			-26						188	114			
		6				90		822			-17						172	93			
		7				83		704			-10						161	58			
		8				90		591			17						154	28			
		9				92		477			36						163	4			
		10				85		371			15						176	-7			
		11				80		259			38						196	-9			
		12				58		161			84						337	132			
		13				-134		-159			-278						62	-312			
		14				63		70			-46						289	68			

[a]Dashes in data denote that the instrument failed or was deemed unreliable; blanks denote that the instrument was not used; and negative signs indicate compression.

TABLE IV.- MODEL STRAIN HISTORIES - Concluded

Model	Test	t, sec	Strain, microinches per inch, at strain-gage location[a] -																				
			1	22	3	4	5	6	7	8	9	10	11	12	13	14	15	16	17	18	19	20	21
MW-17	1	0	-4	-13	0	15	22	0	-7	-29	-6	-18	4	17						0	15		11
		1	387	-228	165	191	-155	129		76	-52	-47	-156	144						125	-120		-11
		2	340	-287	251	543	225	62		51	-119	-251	-141	267						91	210		-78
		3	312	-462	233	805	208	42		-44	-208	-402	-170	275						77	220		-85
		4	186	-143	196	897	185	15	-304	-202	-233	-493	-168	264						62	212		-91
		5	111	-129	131	892	159	-23	-306	-364	-260	-552	-202	239						45	170		-33
		6	254	-529	151	847	138	-44	-260	-447	-245	-561	-226	243						45	168		6
		7	239	-291	645	779	112	-108	-304	-533	-237	-564	-252	241						114	152		26
		8	162	-291		711	123	-171	-314	-643	-165	-566	-274	213						-12	162		46
		9	214	-150		622	152	-198	-273	-504	-10	-533	-278	206						0	224		74
		10	254	-86		536	161	-181	-246	-383	31	-524	-285	174						18	228		126
		11	350	-361		460	238	-108	-154	-179	148	-488	-280	116						161	266		150
		12	192	-162		390		-194	-231	-162	66	-481	-313	80						164	264		179
		13	256	-106		306		185	-662	274	231	-373	-300	39						351	741		205
		14	378	8		197		71		312	299	-282	-256	-19						378	322		277
		15	587	175		99		196		510	389	-260	-263	-146						423			244
	2	0	2	-15	-4	0		2	-16	-17	-34	-4	-12	5	209					-4	-7		-23
		1	385	-240	52	271		55		80	-54	-153	-74	252	475					22	74		-110
		2	331	-209	89	592		26		68	-204	-154	-101	305	666					93	55		-166
		3	303	-249	165	814		4		16	-221	-548	-125	305	731					122	44		-110
		4	281	-211	186	906		-4		-17	-212	-642	-146	293	731					135	52		-94
		5	238	-200	-2	910		-38		-14	-214	-705	-166	286	718					139	23		-135
		6	297	-238	-227	887		-56		-30	-236	-748	-182	277	677					117	30		-107
		7	270	-198	-322	833		-89		-31	-115	-790	-187	235	615					104	22		-86
		8	229	-225	-395	772		-144		35	-59	-817	-212	236	559					75	-8		-24
		9	218	-267	-442	709		-186		26	-78	-851	-237	236	495					40	-28		-28
		10	202	-273	-480	653		-133		30	-30	-851	-207	222	439					9	-20		-24
		11	217	-253	-490	588		-122		10	24	-893	-182	201	385					4	49		21
		12	231	-320	-479	487		75		278	95	-982	-94	219	316					20	166		58
		13	201	-262	-448	388		-15		71	340	-881	512	319	236					36	75		12
		14	358	185	-448	337		-44		76	115	-787	-56	139	205					57			383
		15	329	-80	-442	239		71															77
MW-18	1	0	18	-4		-21		20	23		-7	-37	9	-7	-13	-225			8	-14	22	-2	-7
		1	375	-93		26		285	-86		-40	-126	248	-108	240	-497			83	20	101	-143	-61
		2	256	-312		-122		616	318		-99	-264	56	240	248	-524			140	18	103	-181	-40
		3	279	-276		-166		861	350		-203	-411	12	248	201	-381			171	28	99	-170	37
		4	39	-316		-155		909	343		-238	-458	-21	201	153	-265			193	26	78	-170	7
		5	-107	-445		-122		892	306		-261	-519	-39	153	122	-123			208	-12	62	-179	94
		6	-122	-171		-103		834	197		-186	-556	-55	122	110	-30			211	-46	99	-181	64
		7	-172	-52		-96		758	234		-144	-590	-62	110	94	18			217	-57	120	-98	117
		8	-193	-47		-78		672	265		-66	-617	-51	94	78	55			222	-75	132	-25	120
		9	-206	44		-66		578	238		-72	-576	-60	78	59	120			201	18	236	84	146
		10	-213	24		-54		502	227		-20	-563	-76	59	35	161			193	24	248	125	167
		11	-234	33		-59		416	193		-7	-620	-95	35	-16	195			189	218	363	165	173
		12	-286	109		-80		329	356		18	-780	-102	-16	-122	225			239	1145		157	195
		13	-345	171		-5		193	645		-88	-399	-210	62					254	----			2
		14	-164	94		129		127			96	-536	-86	-154					506	----			186
		15	-274	381		-2		-180															
	2	0		-21		-34		18			-53	5	-19	8					3			-21	-22
		1		-42		-49		345			-205	175	114	373					2			-72	-36
		2		-335		-110		714			-418	90	324	737					63			-107	-143
		3		-291		-134		965			-555	21	324	858					114			-181	-534
		4		-217		-131		1040			-653	-28	312	1089					147			-256	-109
		5		-101		-83		1027			-709	-36	282	1081					177			-325	-72
		6		72		-39		953			-735	-40	249	1008					199			-374	-24
		7		261		-8		833			-758	-48	243	901					220			-423	-3
		8		316		19		732			-768	-43	220	789					255			-439	41
		9		251		41		634			-775	-42	210	682					285			-467	60
		10		293		58		551			-789	-33	194	572					309			-479	78
		11		494		53		461			-671	-24	165	461					324			-472	87
		12		512		36		361			-858	-5	57	374					348			-493	143
		13		473		15		253			-862	42	66	307					609			-395	145
		14		491		134		163			-725	54	55						669			-402	136
		15				88		94			-822	48										-435	

[a]Dashes in data denote that the instrument failed or was deemed unreliable; blanks denote that the instrument was not used:, and negative signs indicate compression.

TABLE V.- SUMMARY OF MODEL BEHAVIOR

(a) Description of model-vibration tests

Model	Test	Model vibration
MW-4-(2)	1	65-cps bending and torsion after starting disturbances; 130-cps random vibration at 8.7 seconds; 80-cps torsion at 10.7 seconds; 173-cps torsion after tip-stabilizer reentry
	2	72-cps vibration after starting disturbances; 238-cps flutter until destruction between 7.32 seconds and 7.68 seconds
MW-16	1	60- to 78-cps random vibrations throughout test
	2	275- to 286-cps random vibrations throughout test; 60-cps vibration before shutdown disturbances
	3	258- to 266-cps random vibrations throughout test
	4	60-cps vibration at 9 seconds
MW-17	1	130- to 140-cps vibrations throughout test; 140-cps torsion after tip-stabilizer reentry
	2	140-cps torsion after tip-stabilizer reentry
MW-18	1	145-cps bending and torsion after tip-stabilizer reentry
	2	70-cps vibration from 5 seconds until shutdown; 124- and 70-cps torsion after tip-stabilizer reentry

(b) Approximate times for particular events

Approximate time, sec	Stagnation pressure, psia	Model condition
0 to 1.2	<50	Violent model buffeting
1.7 to 11.5	>100	Test conditions exist
1.7 to 11.0	----	Tip stabilizer out of airstream
13.4 to end	<50	Violent model buffeting
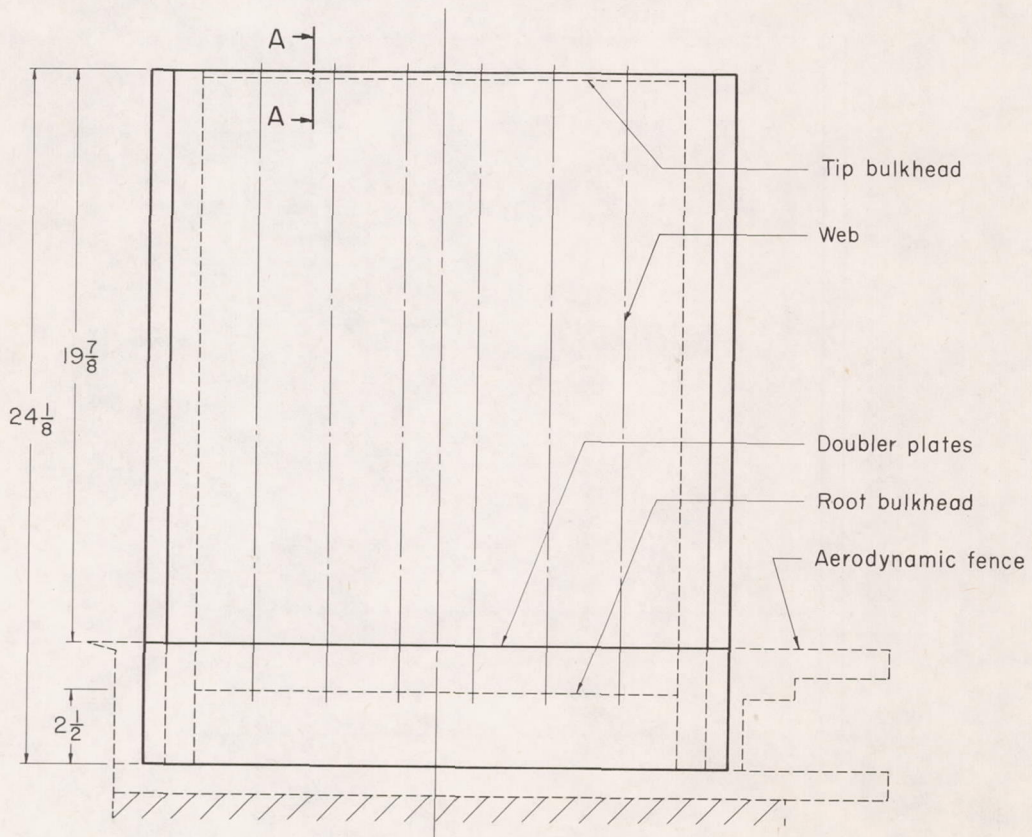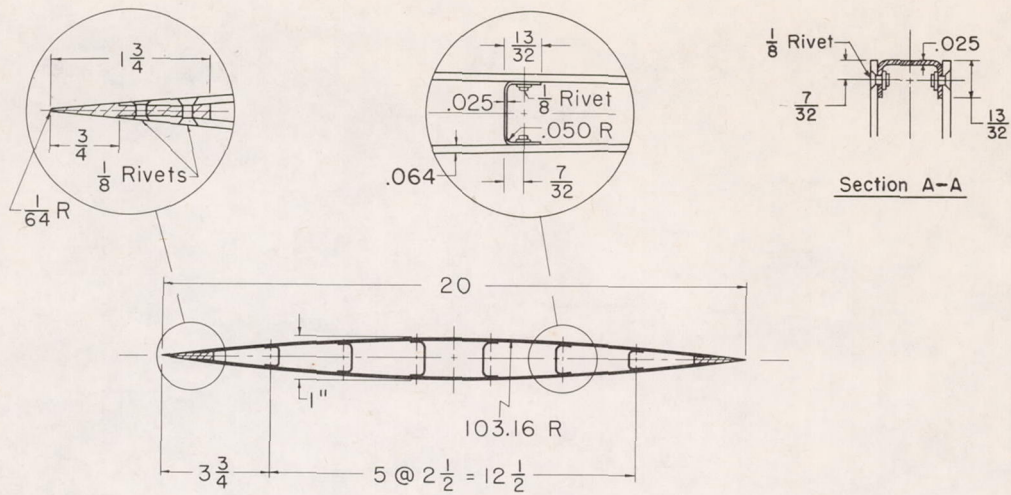
(a) Model MW-4-(2).

Figure 1.- Construction of multiweb wing models. All dimensions are in inches.
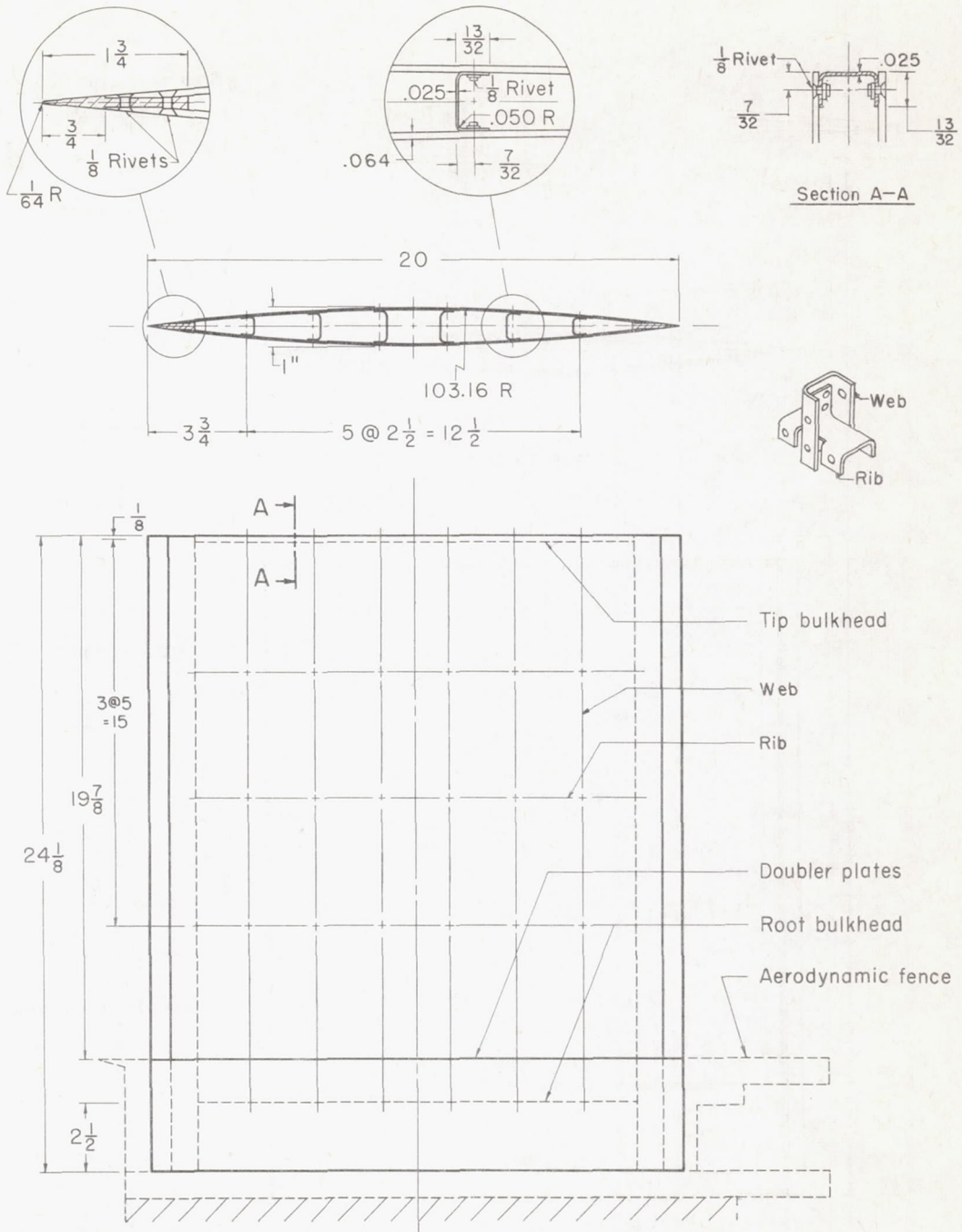
(b) Model MW-16.

Figure 1.- Continued.
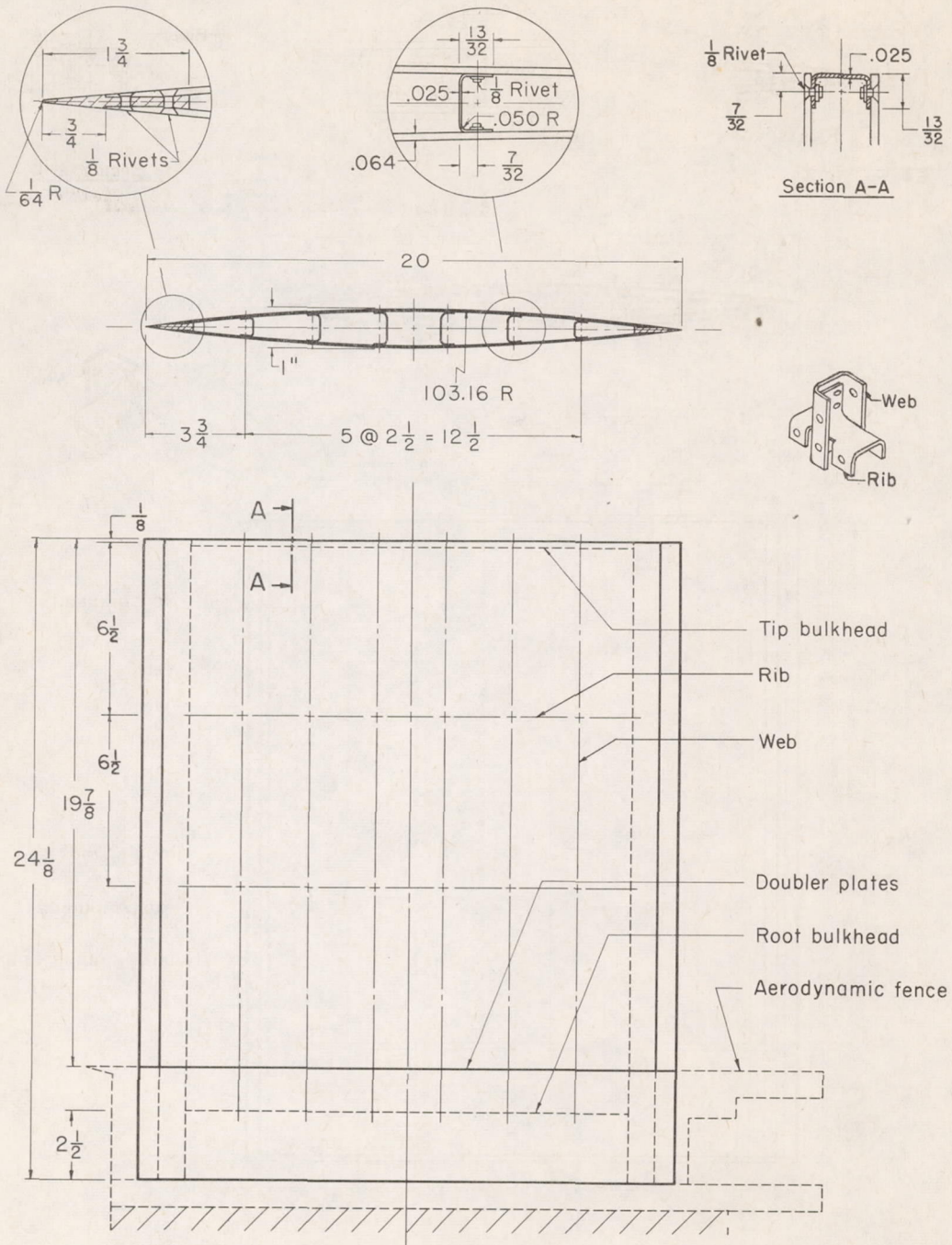
(c) Model MW-17.

Figure 1.- Continued.
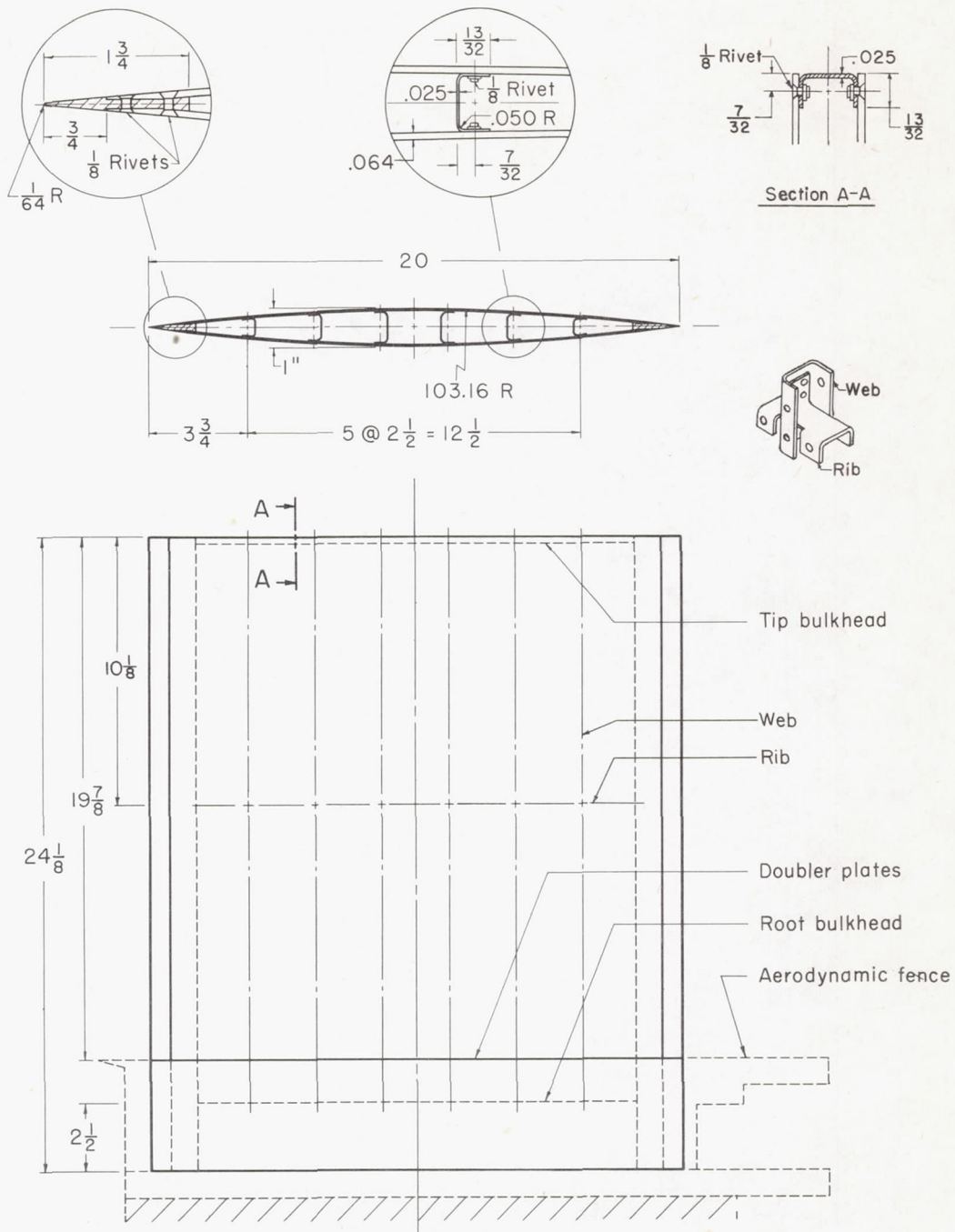
(d) Model MW-18.

Figure 1.- Concluded.
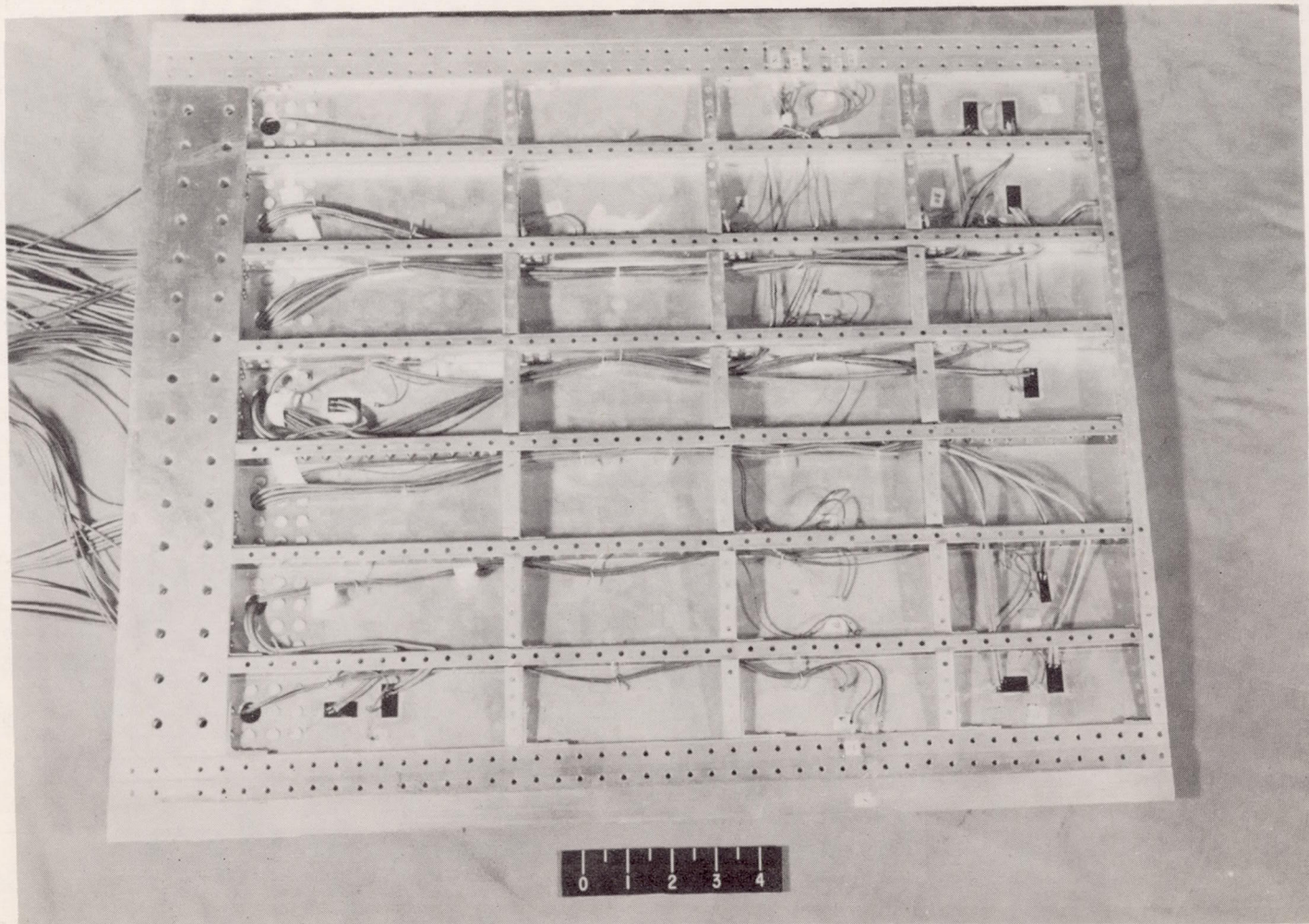
L-80729.1

Figure 2.- Photograph showing installed instrumentation in interior of
model MW-16 prior to final assembly.
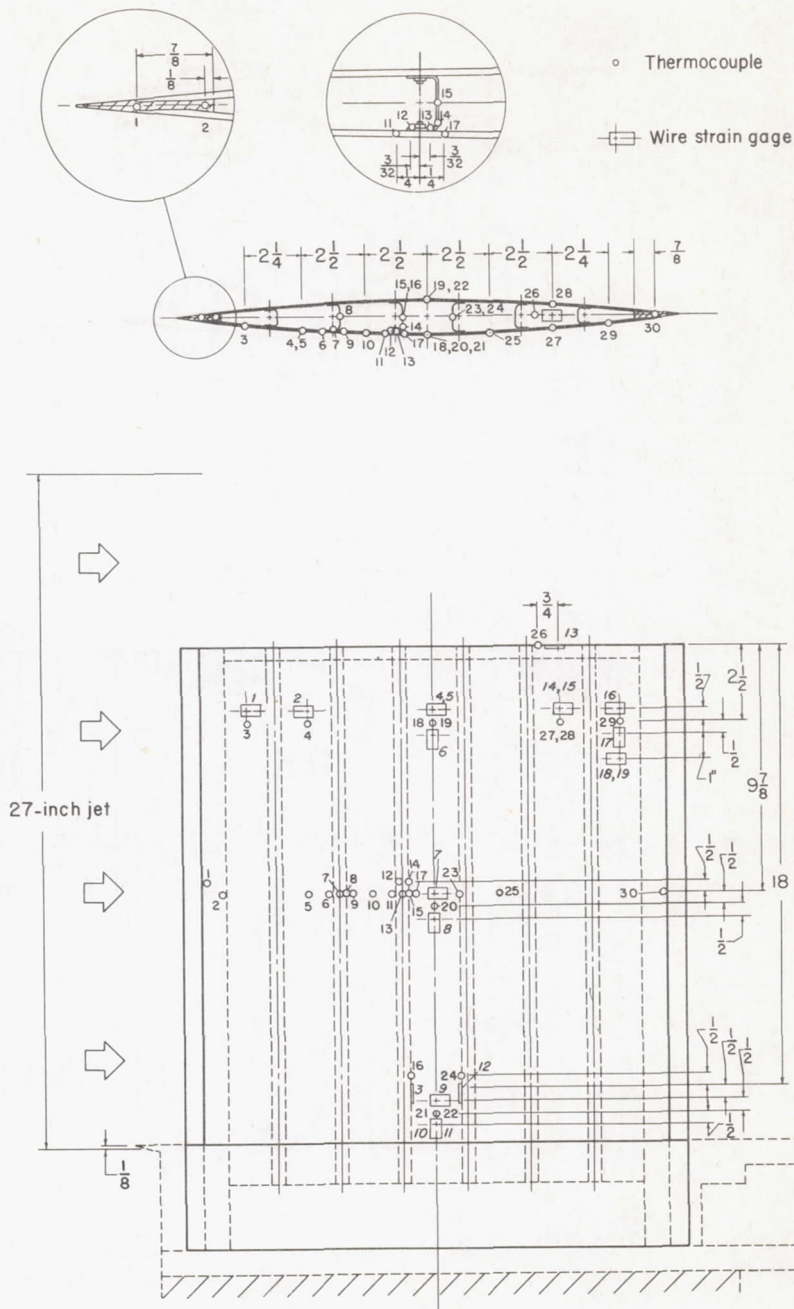
(a) Model MW-4-(2).

Figure 3.- Location of instrumentation of multiweb wing models. Where two wire strain gages are listed, the second is on the far skin.
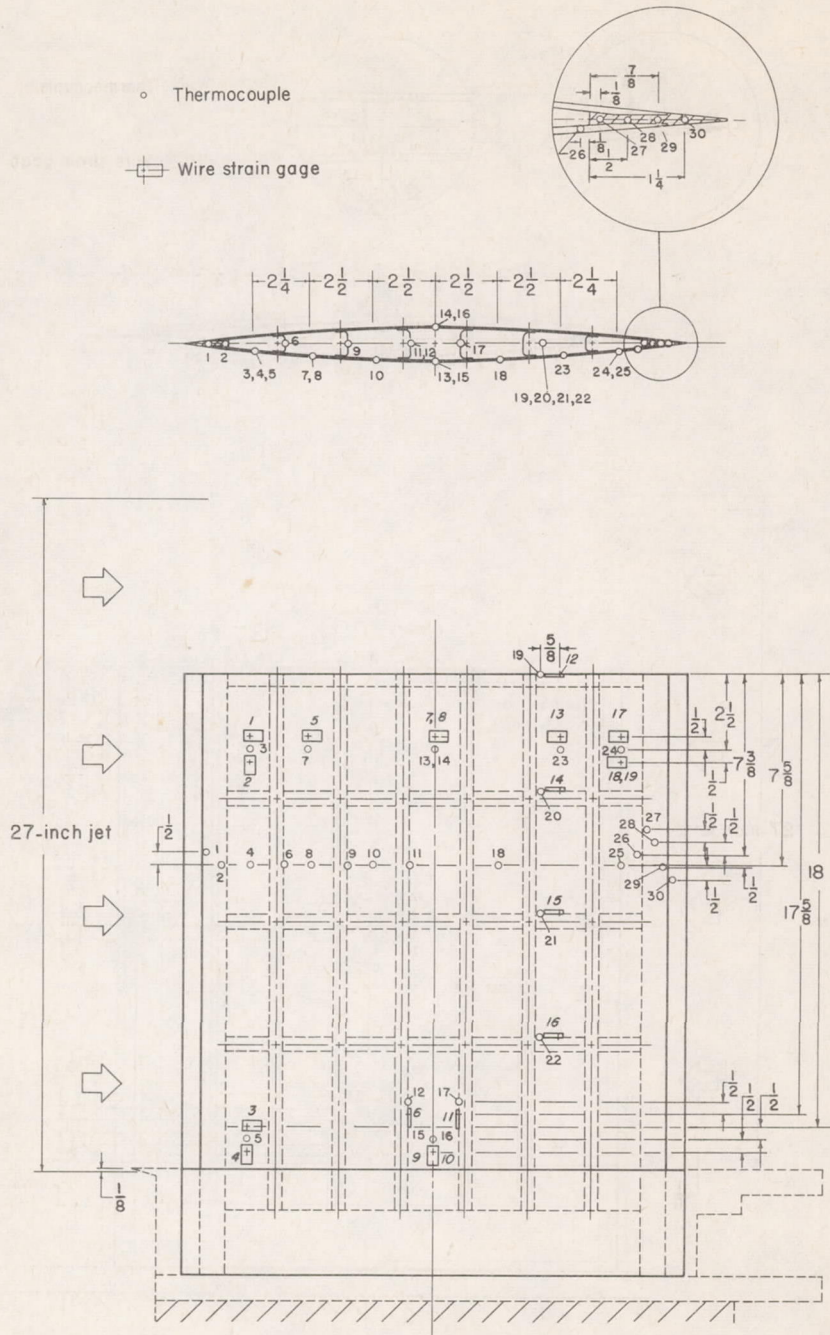
(b) Model MW-16.
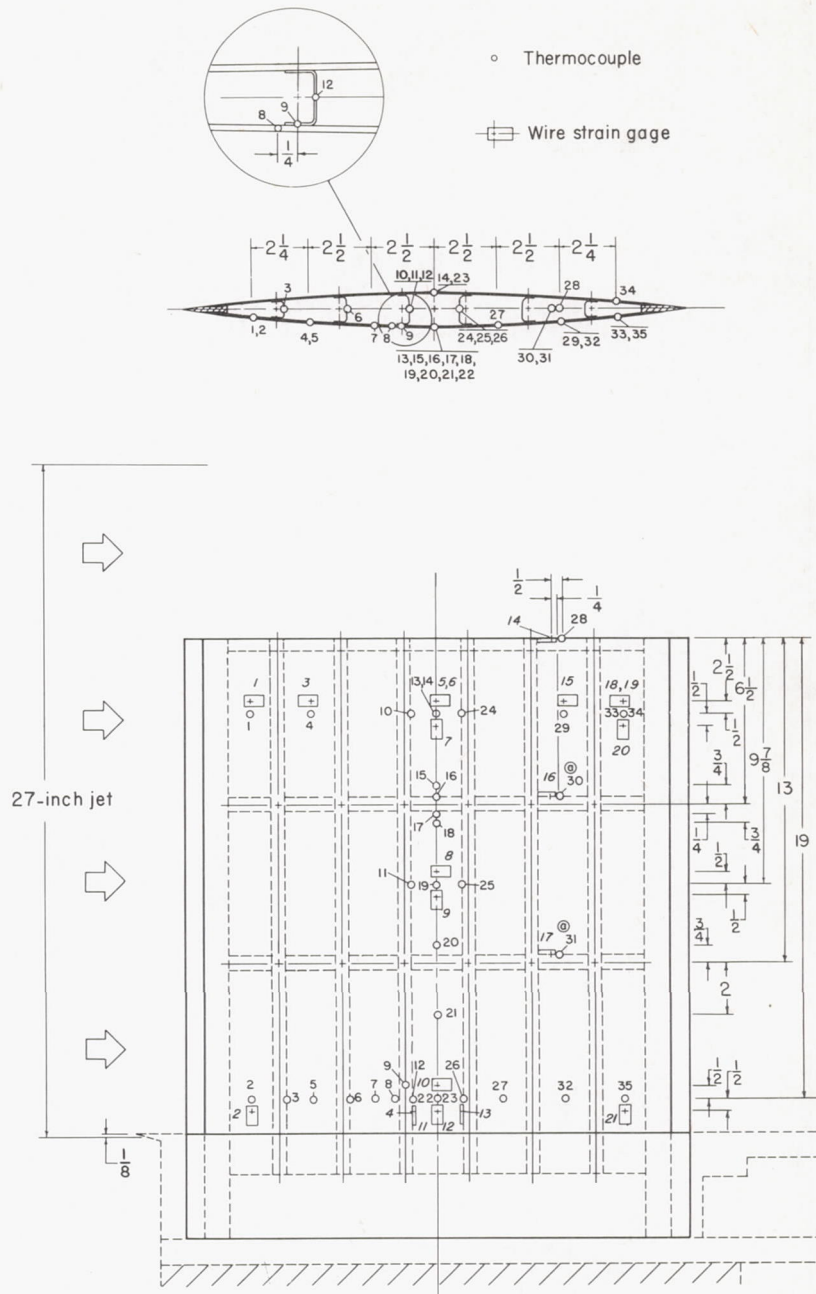
Figure 3.- Continued.

(c) Model MW-17. The symbol (a) denotes a dimension of 3/8 inch
between thermocouple and wire-strain-gage center line.

Figure 3.- Continued.

○ Thermocouple

⊞ Wire strain gage
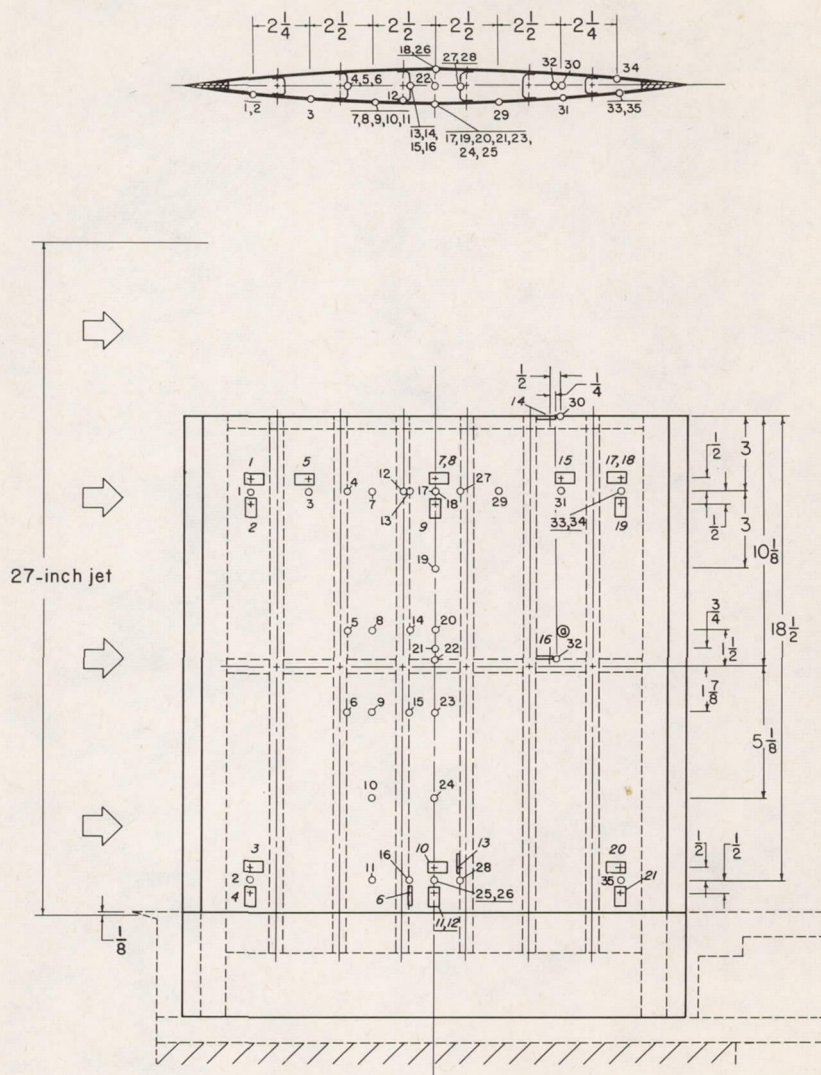
(d) Model MW-18. The symbol ⓐ denotes a dimension of 3/8 inch between thermocouple and wire-strain-gage center line.

Figure 3.- Concluded.
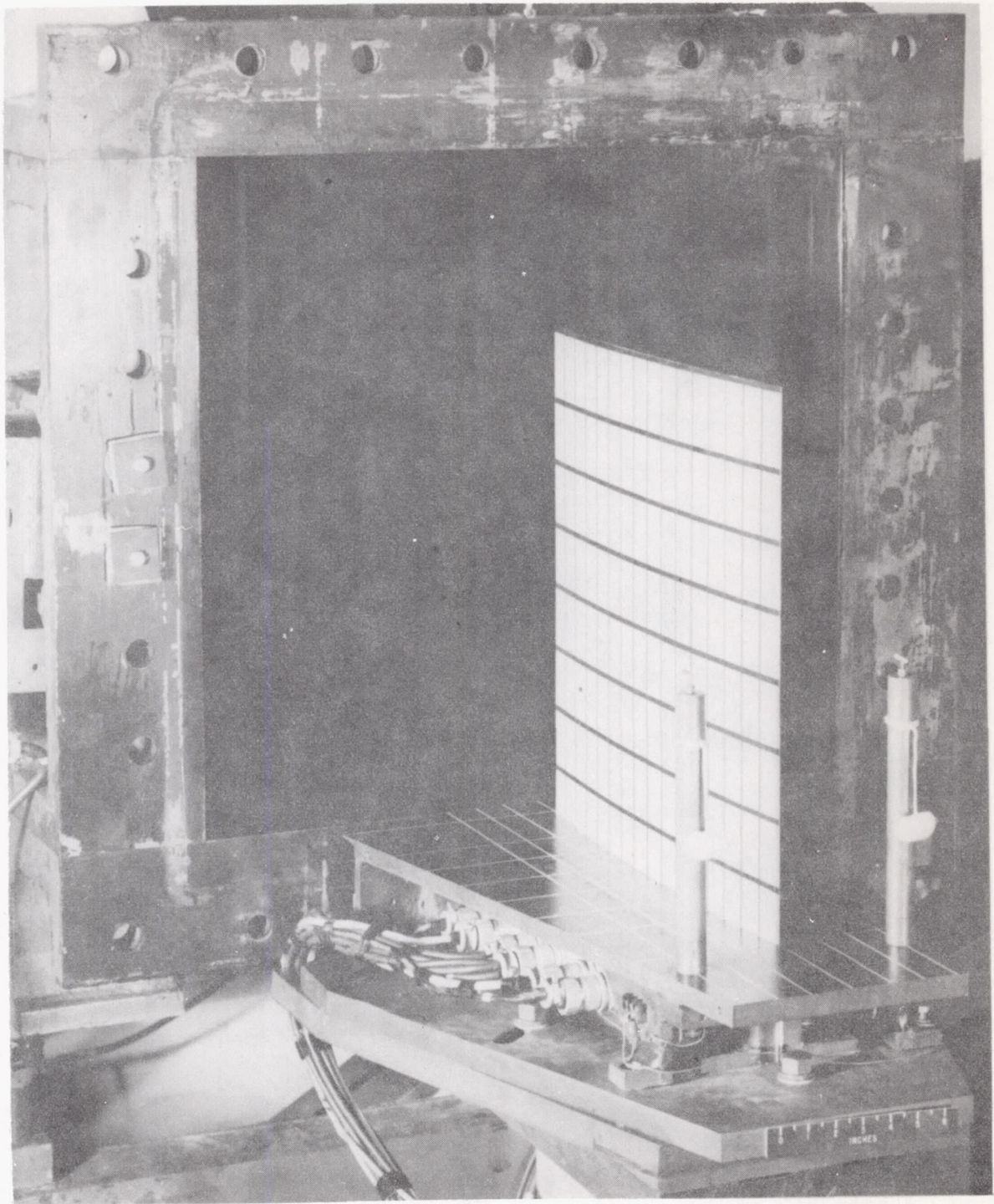
Figure 4.- Model in place at nozzle exit prior to test. L-81922
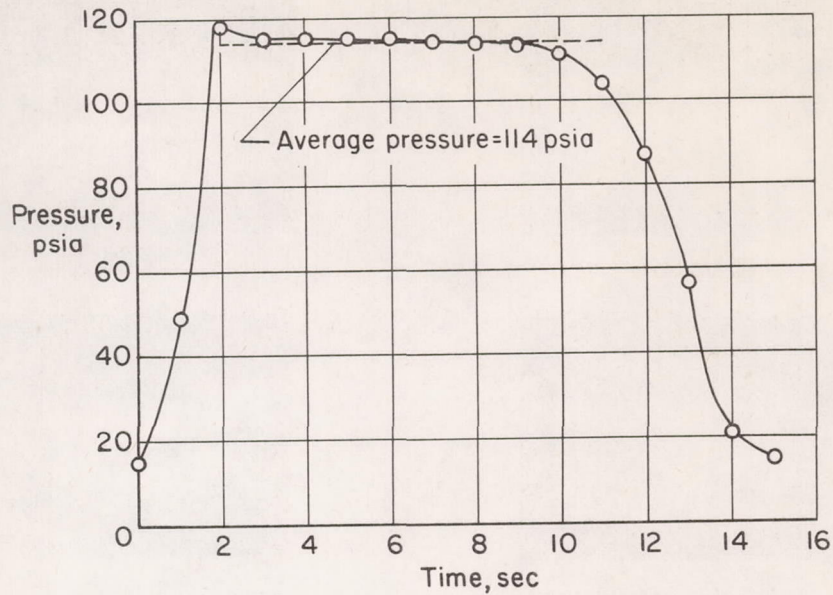
Figure 5.- Typical variation of stagnation pressure with time.
Model MW-18; test 1.
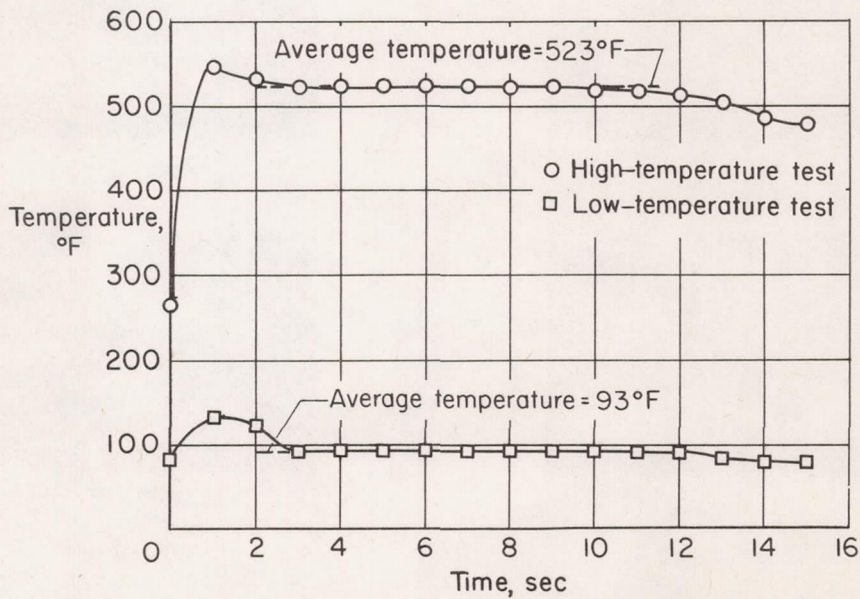
Figure 6.- Typical variation of stagnation temperature with time.
Elevated-temperature test data are from test 1 of model MW-18;
low-temperature test data are from test 1 of MW-4-(2).

7.620 SEC

7.622 SEC

7.650 SEC

7.652 SEC

7.661 SEC

7.663 SEC

7.671 SEC

7.675 SEC
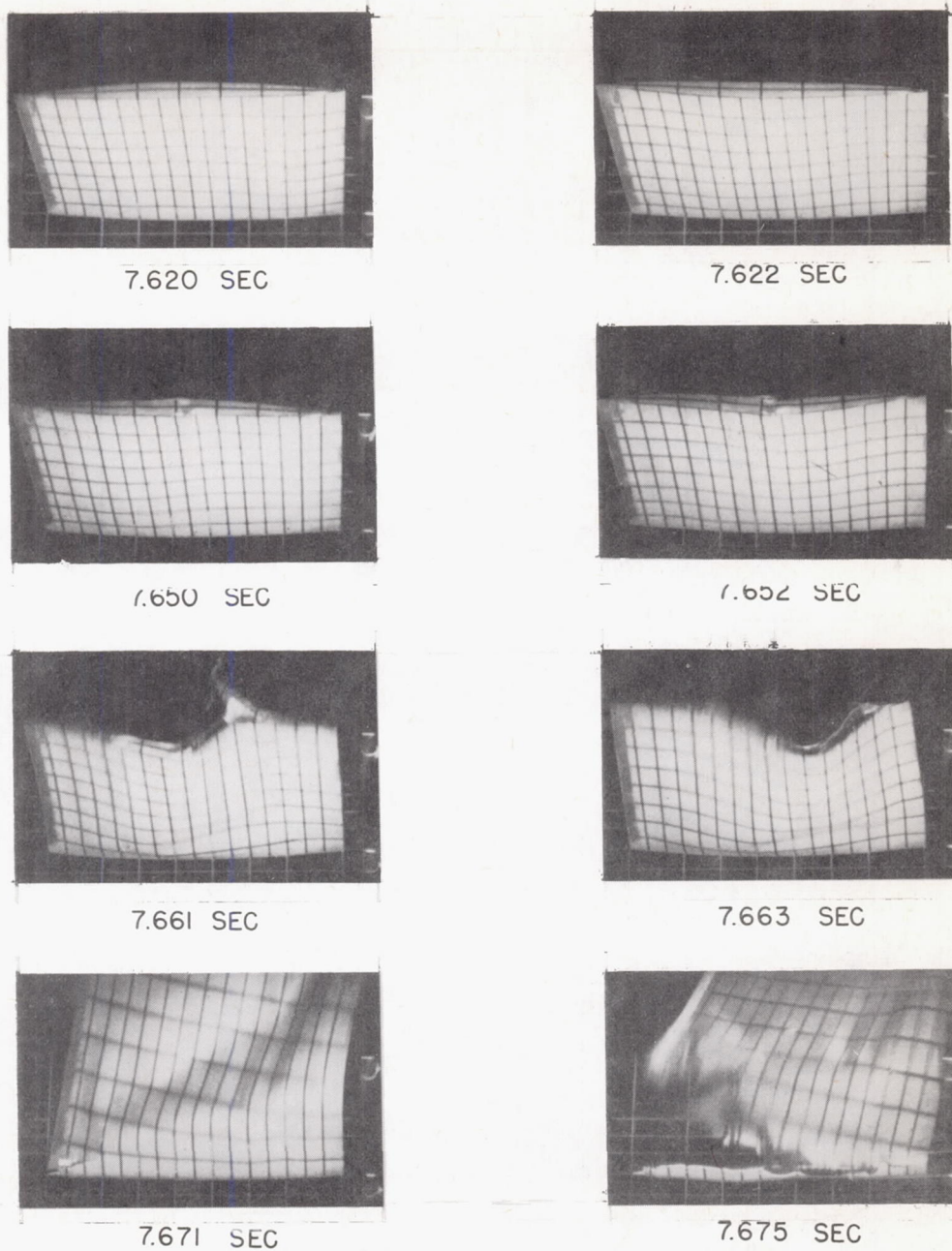
L-57-4443

Figure 7.- Flutter and failure sequence of model MW-4-(2) at α = 0°.
Flutter frequency, 240 cps; air flows from left to right.
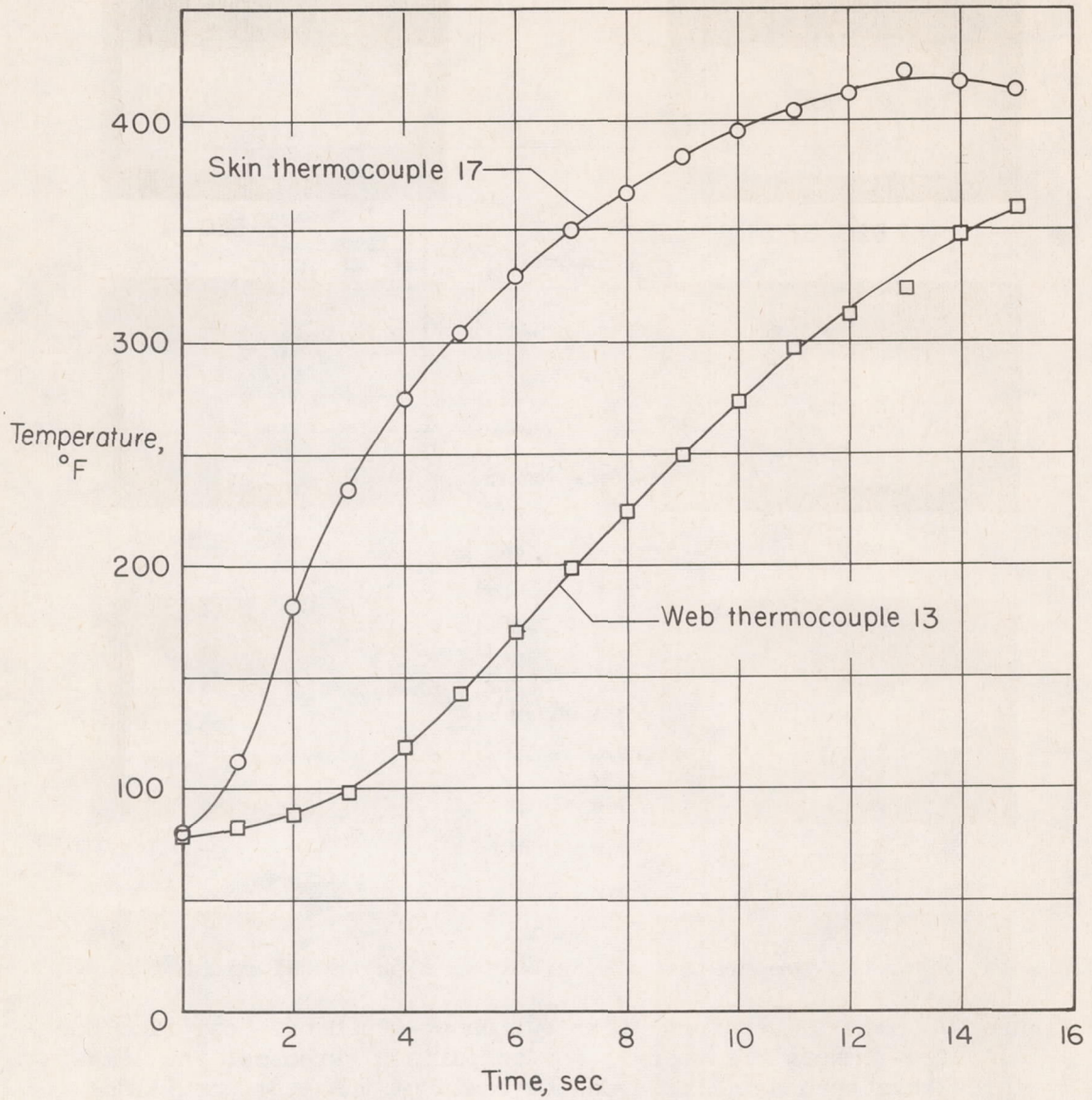
Figure 8.- Typical model temperature histories during a high-stagnation-
temperature test. Model MW-18; test 1.

(a) Spanwise temperature distribution along model midchord.

Figure 9.- Skin-temperature distribution at 6 seconds test time for elevated-temperature tests. For comparison purposes, the temperatures have been normalized on the basis of the test conditions experienced by model MW-18 during test 1.
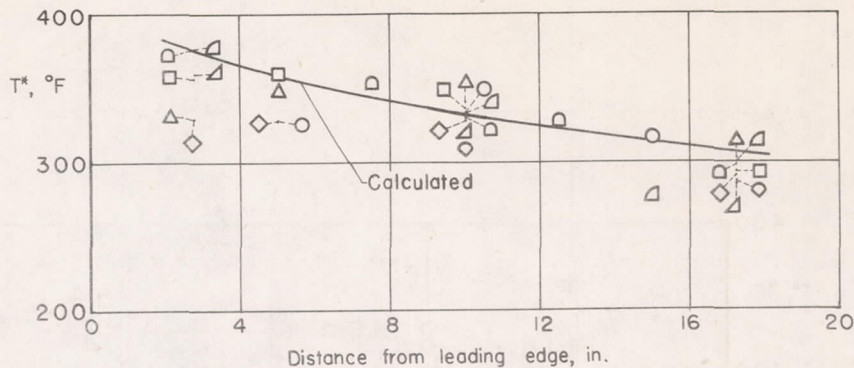
(b) Chordwise temperature distribution at approximately 17.25 inches from the root.
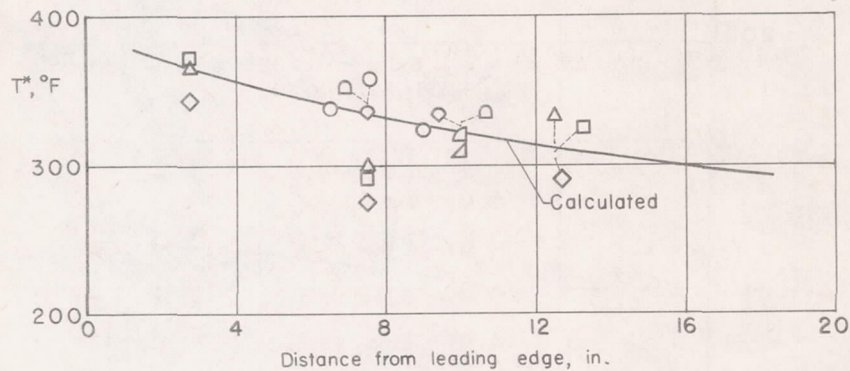
(c) Chordwise temperature distribution at approximately the midspan.
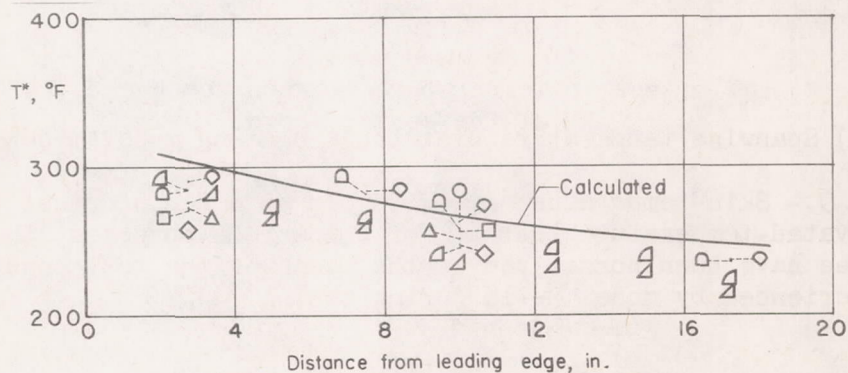
(d) Chordwise temperature distribution at approximately 2 inches from the root.

Figure 9.- Concluded.
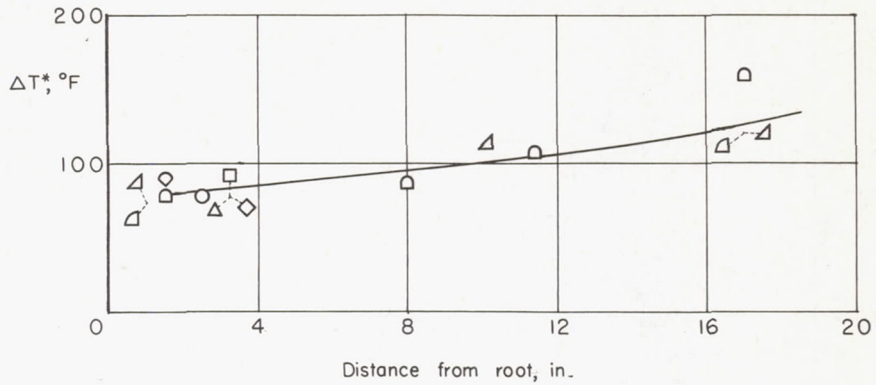
(a) Difference in temperature between web 3 and the skin
at the midchord.
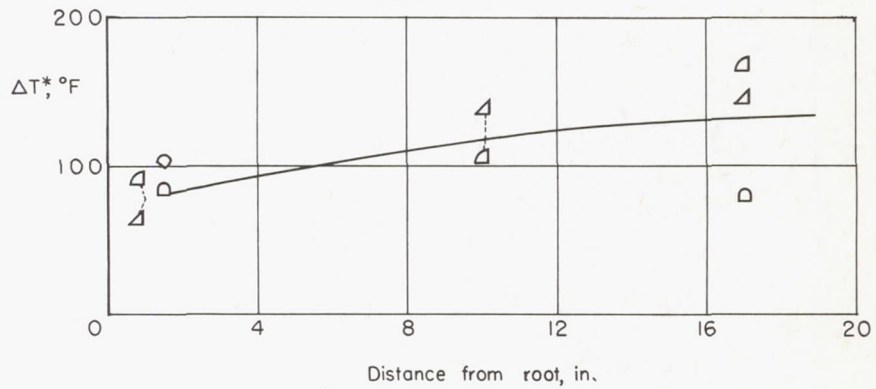
(b) Difference in temperature between web 4 and the skin
at the center chord.

O MW-4-(2), test no. 2   ⊿ MW-17, test no. 1

□ MW-16, test no. 2   ⊿ MW-17, test no. 2

◇ MW-16, test no. 3   ▢ MW-18, test no. 1

△ MW-16, test no. 4   ◇ MW-18, test no. 2

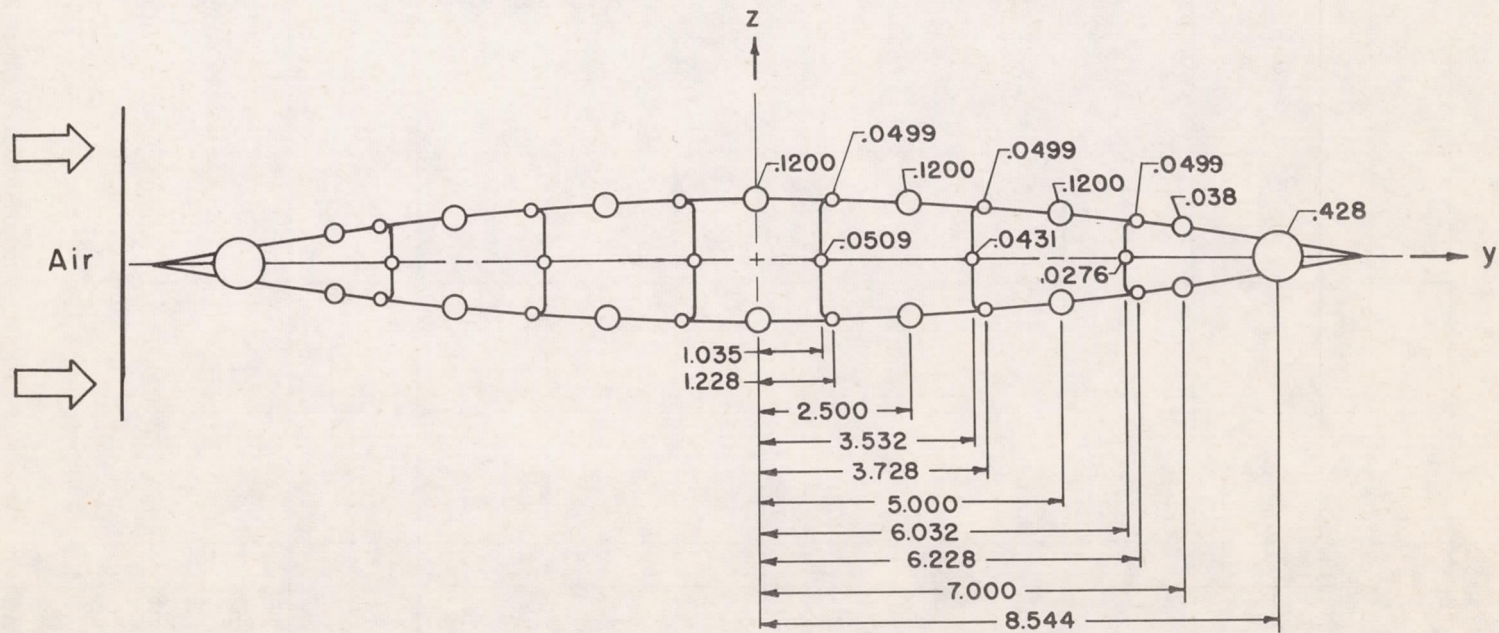Figure 10.- Difference between skin temperatures and web temperatures
at 6 seconds test time.

Figure 11.- Idealized cross section used to calculate thermal stresses from the experimental temperature distribution. The cross section is geometrically doubly symmetric.
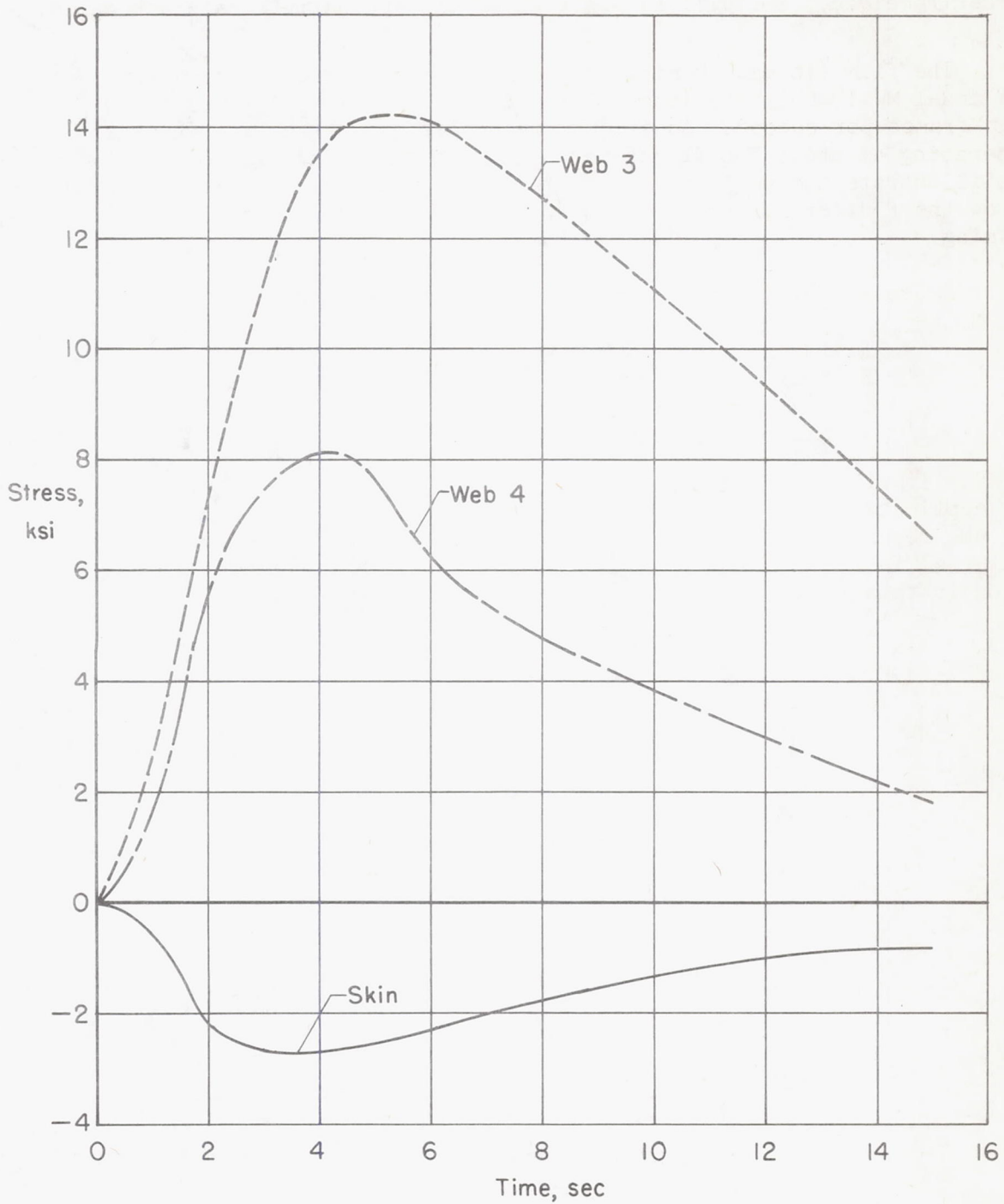
Figure 12.- Calculated stresses about the midchord at a section 3 inches from the tip of model MW-18 during test 1.